

PARTICLES, ENVIRONMENTS, AND POSSIBLE ECOLOGIES IN THE JOVIAN ATMOSPHERE

CARL SAGAN AND E. E. SALPETER

Center for Radiophysics and Space Research, Cornell University

Received 1975 December 11; revised 1976 June 1

ABSTRACT

The eddy diffusion coefficient is estimated as a function of altitude, separately for the Jovian troposphere and mesosphere. The growth-rate and motion of particles is estimated for various substances: the water clouds are probably nucleated by NH_4Cl , and sodium compounds are likely to be absent at and above the levels of the water clouds. Complex organic molecules produced by the $L\alpha$ photolysis of methane may possibly be the absorbers in the lower mesosphere which account for the low reflectivity of Jupiter in the near-ultraviolet. The optical frequency chromophores are localized at or just below the Jovian tropopause. Candidate chromophore molecules must satisfy the condition that they are produced sufficiently rapidly that convective pyrolysis maintains the observed chromophore optical depth. Organic molecules and polymeric sulfur produced through H_2S photolysis at $\lambda > 2300 \text{ \AA}$ probably fail this test, even if a slow, deep circulation pattern, driven by latent heat, is present. The condition may be satisfied if complex organic chromophores are produced with high quantum yield by NH_3 photolysis at $\lambda < 2300 \text{ \AA}$. However, Jovian photoautotrophs in the upper troposphere satisfy this condition well, even with fast circulation, assuming only biochemical properties of comparable terrestrial organisms. Unless buoyancy can be achieved, a hypothetical organism drifts downward and is pyrolyzed. An organism in the form of a thin, gas-filled balloon can grow fast enough to replicate if (i) it can survive at the low mesospheric temperatures, or if (ii) photosynthesis occurs in the troposphere. If hypothetical organisms are capable of slow, powered locomotion and coalescence, they can grow large enough to achieve buoyancy. Ecological niches for sinkers, floaters, and hunters appear to exist in the Jovian atmosphere.

Subject headings: planets: atmospheres — planets: Jupiter

I. INTRODUCTION

The contemporary Jovian atmosphere has some similarities to the primitive terrestrial atmosphere, where organic molecules were produced readily; and experiments in which a wide variety of organic molecules are produced under conditions similar to those of the Jovian atmosphere have been carried out (Sagan and Miller 1960; Sagan *et al.* 1967; Woeller and Ponnampertuma 1969; Rabinowitz *et al.* 1969; Sagan and Khare 1971*a, b*; Khare and Sagan 1973; Ferris and Chen 1975). This has led to the hypothesis that there may be a Jovian biology (Sagan 1961; Shklovskii and Sagan 1966). Observations in the visible and in the ultraviolet have implied the presence of particulate matter in the Jovian atmosphere which may (but need not necessarily) be connected with questions of Jovian organic chemistry and biology. Both chemical and biological issues are affected by fluid dynamics in the Jovian atmosphere. We are here concerned largely with these effects.

Modern models of the structure of Jupiter (for references, see, e.g., Stevenson and Salpeter 1976) predict that the bulk constituent, a hydrogen-helium mixture, is fluid throughout, with temperatures increasing inward to above 10^4 K . Plausible organisms require temperatures well below 10^3 K . One principal

problem which must be faced by such hypothetical organisms is descent to pyrolytic depths due either to the acceleration of gravity or to convective downdrafts. The second half of the present paper examines (1) whether such organisms undergo significant growth and replication in less than the time scale for drift to pyrolytic depths, or (2) whether other adaptations to avoid pyrolysis are hydrodynamically and biologically feasible. We shall see that (1) becomes easier for smaller organisms and (2) for larger ones.

That plausible and internally consistent Jovian ecologies can be described cannot, by itself, demonstrate the likelihood of life on Jupiter. A tenable argument for life on Jupiter must also show that the origin of life on that planet was possible. Since many steps, particularly the later ones, which led to the origin of life on Earth are only incompletely understood (see, e.g., Miller and Orgel 1973), a thorough discussion of the origin of life on Jupiter cannot be undertaken at the present time. Most skepticism on this subject seems to arise from the contention that synthesized molecules will be carried convectively to pyrolytic depths before the origin of life can occur. The unspoken premise in such an argument is that pyrolysis would not have occurred on the primitive Earth. However, the measured Arrhenius rate constants imply, through a regression analysis, that many

essential organic molecules, for example a number of biological amino acids, suffer thermal degradation at typical terrestrial surface temperatures in geologically short time periods. The very limited available experimental data show, for example, that the half-life at 30° C of the amino acid serine is $\sim 10^4$ yrs and of threonine is $\lesssim 10^5$ yrs; while at the same temperature the half-life of the simplest amino acid, alanine, is $> 10^{10}$ yrs (Vallentyne 1964). Because of the exponential Arrhenius kinetics, the highest temperatures on a temperature-variable planet dominate the net molecular degradations; also there is evidence that aqueous solution and alkaline pH's—both expected on the primitive Earth—enhance the decomposition rates (Vallentyne 1964). It does not seem at all improbable that some essential precursor molecules for the origin of life had half-lives on the primitive Earth of 10^2 to 10^3 yrs, not greatly dissimilar to the lifetimes against convective pyrolysis of organic molecules on contemporary Jupiter, as calculated below.

Many workers on the origin of life have suggested that the rate-limiting steps were stochastic in nature. The volume available for natural molecular experiments on Jupiter is approximately 10^3 times larger than on Earth. If phase interfaces play a critical role in the origin of life (see, e.g., Bernal 1973) Jupiter, with a great concentration of solid and liquid atmospheric aerosol particles, would be particularly favorable.

The origin of life on Earth took a period < 0.1 the lifetime of the Earth, and possibly much less (Sagan 1975). On Jupiter, we have much longer periods of time available for chemical experiments, a larger interaction volume, and a much larger area for phase interface chemistry. On the other hand, the thermal degradation time scales are shorter for many molecules, and there is a much greater excess of molecular hydrogen than on the primitive Earth, where H_2 was rapidly depleted during planetary formation and in subsequent Jeans escape. The effect of molecular hydrogen on prebiological organic chemistry is inadequately understood, but is briefly discussed below. Its effect on quenching gas-phase organic reactions is less than linear, at least for some reactions. We conclude that the absolute *a priori* likelihood of life on Jupiter, as on Earth, cannot be estimated reliably at the present time, but, as on Earth, can hardly be ruled out. The relative *a priori* probabilities of the origin of life, in a comparison of Jupiter and Earth, depend on which reactions and molecular precursors are rate-limiting. If, for example, the alanine abundance is rate-limiting, the Earth is strongly favored; if serine is rate-limiting, Jupiter may be favored. It is also possible that there exists a variety of different paths to the origin of life, for some of which the Earth is favored and for others of which Jupiter is favored.

We devote the remainder of the present paper to a characterization of the relevant physical environment of Jupiter; to a discussion of the chromophores responsible for the observed coloration of the planet; and to an analysis of some permissible ecological niches of hypothetical Jovian organisms.

Values for the eddy diffusion coefficient K play an important role in such arguments. Estimates are given in § II, separately for the convective troposphere and for the more stable mesosphere. Analytic approximations are also given there for abundance as a function of height for particles which are produced at some upper level and are transported downward toward pyrolysis.

We are concerned with two sorts of particulate matter: particles that condense out under conditions of thermal equilibrium, and particles that require an investment of free energy for their production. Equilibrium condensation has been studied previously for H_2O , NH_4SH , and NH_3 ; we investigate it further in § III for a number of substances with higher condensation temperatures. We estimate growth rates for these condensates and discuss whether NaCl or other particles can be present at the level of the water clouds to act as nucleation agents. The production of chromophores and of nonequilibrium organic molecules is treated in § IV. We obtain a lower limit to the production rate of ethane from methane photolysis by solar $L\alpha$, and treat organic chromophores produced by various wavelengths of light, as well as polymeric sulfur chromophores.

The motion of hypothetical organisms is discussed in § V, and the diffusion of metabolites and the consequent growth of organisms in § VI. We consider four different cases, depending on whether organisms can or cannot survive at the low temperatures of the mesosphere and whether they can or cannot utilize visible light for photosynthesis. In § VII we consider the more rapid growth attainable if organisms can control their motions.

II. EDDY DIFFUSION IN THE JOVIAN ATMOSPHERE

The total infrared flux emerging from Jupiter (Aumann, Gillespie, and Low 1969; Ingersoll *et al.* 1975) is $F_{\text{tot}} \equiv \sigma T_{\text{eff}}^4 \approx 1.5 \times 10^4$ ergs $\text{cm}^{-2} \text{s}^{-1}$ ($T_{\text{eff}} \approx 127$ K), with about half of this flux coming from the deep interior ($F_{\text{int}} \approx 0.8 \times 10^4$ ergs $\text{cm}^{-2} \text{s}^{-1}$). The radiative opacity increases fairly rapidly with increasing pressure P , and radiative-convective model calculations predict a fairly rapid change across the boundary level defined here as the tropopause. Above the tropopause we have radiative (subadiabatic) heat transport in the mesosphere; below we have convective heat transport (with the temperature gradient only slightly superadiabatic) in the troposphere. Model atmospheres (Trafton and Munch 1969; Hogan, Rasool, and Encrenaz 1969; Wallace, Prather, and Belton 1974) and spectroscopic observations (Gillett, Low, and Stein 1969; Aitken and Jones 1972; Lacy *et al.* 1975) suggest a temperature $T \approx 175$ K at the pressure level of $P = 1$ bar and place the tropopause somewhere slightly above this. We shall adopt the level ($T \approx 145$, $P \approx 0.5$ bar) for the tropopause. These numbers are consistent with *Pioneer 10* infrared radiometer data (Orton 1975a) and with ground-based infrared radiometric measures (Orton 1975b) and possibly also with *Pioneer 10* and *11* S-band occultation data (Kliore and Woiceshyn 1976). We assume a

helium abundance of about 10% by number, consistent with separate measurements from the occultation of Beta Scorpii (Elliot *et al.* 1974); from *Pioneer 10* and *11* ultraviolet photometry (Carlson and Judge 1974); and from the pressure broadening of the $J = 0$ and $J = 1$ hydrogen lines (Houck *et al.* 1975). Assuming a helium abundance of about 10% (by number), it then follows that $\gamma/(\gamma - 1) \approx 3$, where γ is the ratio of specific heats, and that the mean molecular weight $\mu \approx 2.2$. For pressure P , pressure scale height $H = P(dP/dz)^{-1}$, density ρ , and kinematic viscosity ν in the troposphere we adopt

$$\begin{aligned} P &\approx \left(\frac{T}{175 \text{ K}}\right)^3 \text{ bar}; \\ H &\approx \left(\frac{T}{175 \text{ K}}\right) 27 \text{ km}; \\ \rho &\approx \left(\frac{T}{175 \text{ K}}\right)^2 1.6 \times 10^{-4} \text{ gm cm}^{-3}; \\ \nu &\approx \left(\frac{T}{175 \text{ K}}\right)^{-1.5} 0.5 \text{ cm}^2 \text{ s}^{-1}. \end{aligned} \quad (1)$$

In the mesosphere, the temperature gradient decreases rapidly (for $P \leq 0.2$ bar, say), and the minimum temperature is about 120 K followed by a temperature inversion whose structure is not yet well known (possibly $T_{\text{max}} \approx 150$ K at $P \sim 10^{-3}$ bar).

For a general convective circulation pattern the vertical convective heat flux F_c is given by

$$F_c = c_p \rho \Delta T w_c, \quad (2)$$

where c_p is the specific heat at constant pressure, ΔT is the typical vertical excess in the temperature drop, and w_c the typical vertical convection speed. For vertical distances larger than the vertical extent l of the circulation pattern, one has an eddy diffusion coefficient $K_c \equiv w_c l$; and we shall denote by t_c the eddy diffusion time, H^2/K_c , for diffusion through a single pressure scale height H . In the simplest form of Prandtl mixing-length theory (see, e.g., Schwarzschild 1958), the circulation is characterized by two parameters, the mixing length l and the superadiabaticity with w_c^2 and $\Delta T/T$ both proportional to the superadiabaticity. We replace F_c by 1.4×10^4 ergs $\text{cm}^{-2} \text{s}^{-1}$, a typical value for the Jovian troposphere, employ equation (1), and write K_c , w_c , and t_c in the forms

$$\begin{aligned} K_c &= \xi(T/175 \text{ K})^{1/3} \times 10^7 \text{ cm}^2 \text{ s}^{-1}, \\ w_c &= \xi^{1/4}(T/175 \text{ K})^{-2/3} \times 76 \text{ cm s}^{-1}, \\ t_c &= \xi^{-1}(T/175 \text{ K})^{5/3} \times 7.5 \times 10^5 \text{ s}. \end{aligned} \quad (3)$$

In the notation of mixing-length theory our parameter ξ equals $(l/0.05H)^{4/3}$. The Jovian tropospheric lapse rate is then very close to adiabatic ($\Delta T/T \sim 10^{-6}$), as is true by the same argument (Sagan 1960) for all other planetary tropospheres.

In the simplest version of mixing-length theory $l \approx H$ and $\xi \sim 100$. The actual circulation patterns in the troposphere are likely to be much more complex (Hunten 1975). In particular, one should consider the effects of rotation at great depths and of latent heat release in the cloud layers near the tropopause (Gierasch 1973). For a constant value of the heat flux F_c in equation (2), these effects usually increase ΔT and decrease w_c considerably, leading to smaller values of K_c and ξ in equation (3). These considerations suggest, as a simple working hypothesis, $\xi = 1$, which should be accurate to within a factor of about 200.

Gierasch (1976) has suggested a specific large-scale circulation pattern which extends all the way from the bottom of the water-cloud layer ($T \approx 280$ K) to the tropopause. This pattern is driven by the latent heat of water which leads to a relatively large value of $\Delta T/T \sim 10^{-2}$. This corresponds to $\xi \sim 0.01$ with time scales for complete turnover of the region of up to a few years, even though some cloud patterns (above the water clouds) are observed to change in shorter times (Peek 1958). On Gierasch's model, the eddy diffusion coefficient increases by a very large factor just below the cloud bottom to $\xi \sim 10$.

In the mesosphere the bulk of the heat flux F_{tot} is carried by radiation, but some fraction of the flux could drive a circulation pattern working against a subadiabatic temperature gradient. The vertical speed w_m of such a circulation pattern must satisfy an inequality, based on the fact that the adiabatic cooling rate cannot exceed the total available heating rate:

$$H \rho w_m [c_p(dT/dz) + g] \leq F_{\text{tot}}. \quad (4)$$

Except in the immediate vicinity of the tropopause, the temperature gradient in equation (4) can be neglected for the troposphere. Putting $T \approx 150$ K and assuming that the vertical length scale for the circulation pattern is of order H , the eddy diffusion coefficient K_m is of order $w_m H$, so that

$$\begin{aligned} w_m &\leq (1 \text{ bar}/P) 0.016 \text{ cm s}^{-1}; \\ K_m &\leq (1 \text{ bar}/P) 7 \times 10^4 \text{ cm}^2 \text{ s}^{-1}. \end{aligned} \quad (5)$$

Thus typical velocities just below the tropopause are many thousands of times larger than just above the tropopause. Analysis of the observed $L\alpha$ albedo of the upper mesosphere (Wallace and Hunten 1973; Carlson and Judge 1974) indicates $K_m \approx 3 \times 10^{8 \pm 1} \text{ cm}^2 \text{ s}^{-1}$ at levels where $P \approx 3 \times 10^{-7}$ bar; analysis of β Sco occultation measurements (Sagan *et al.* 1974) indicates $K_m > 10^6 \text{ cm}^2 \text{ s}^{-1}$ at similar levels. It is theoretically plausible (French and Gierasch 1974) that gravity-wave propagation upward in the mesosphere contributes to the eddy diffusion. For a single wave mode, K_m has a step-function behavior, but overall it seems plausible to assume some constant fraction of the maximum expression in equation (5). The value given by the $L\alpha$ albedo then suggests

$$K_m \sim (1 \text{ bar}/P) 100 \text{ cm}^2 \text{ s}^{-1}, \quad (6)$$

uncertain by factors of order 10 or 100. Note that

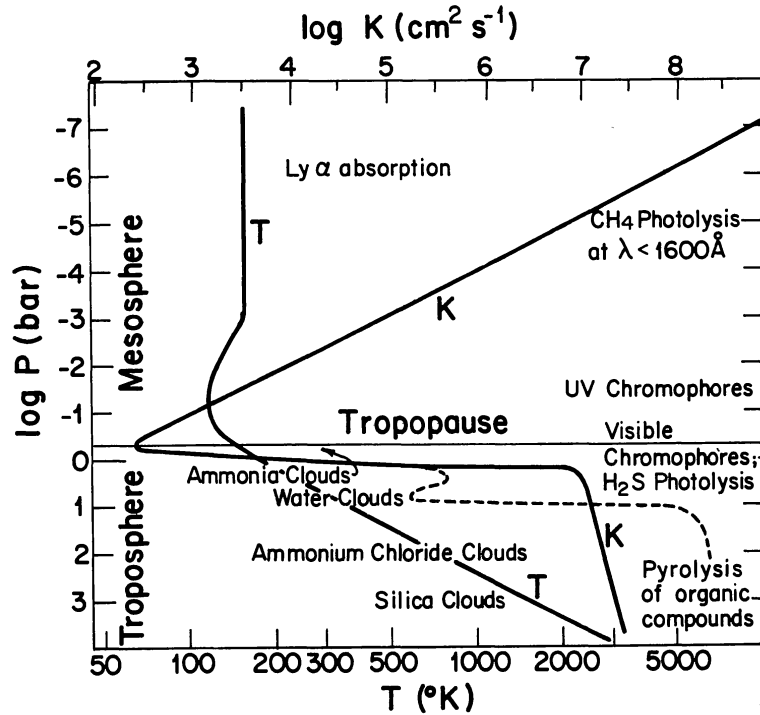


FIG. 1.—A schematic plot of temperature T and eddy diffusion coefficient K versus pressure P for the Jovian atmosphere. The dashed portion of the curve for K corresponds to Gierasch's (1976) model for a deep circulation pattern driven by latent heat effects. Methane photolysis extends upward from the indicated level.

$K_m \propto e^{z/H}$. Temperature T and $K(z)$ are plotted against pressure, schematically, in Figure 1. (The dashed curve for K corresponds to Gierasch's 1976 model in which the latent heat of water condensation is taken into account.)

We shall need continuity equations for $n_j(z)$, the number density as a function of height z of some complex molecule (of molecular weight $\mu_j \gg 2.2$) or of some particle. Let $w_d(z)$ be the steady-state vertical drift velocity of the molecule or droplet falling under gravity through an atmosphere with pressure scale height H , eddy diffusion coefficient K , and mean molecular weight 2.2. In standard notation, the continuity equation (see, e.g., Strobel 1973) reads

$$(K + D_j) \frac{dn_j}{dz} + \left(\frac{K}{H} + \frac{D_j}{H_j} \right) n_j = -\Phi_j,$$

where D_j is the effective molecular (or particle) diffusion coefficient and $H_j = H(2.2/\mu_j) \ll H$ is the effective scale height for the j th particles alone. Φ_j is the vertical flux of particles of species j . H_j and the drift velocity w_d for free fall under gravity are related by $D_j = w_d H_j$. We shall be interested only in levels well below the turbopause where $D_j \ll K$ and give only a simplified version of the standard treatment (Strobel 1973; Prinn 1973). The steady-state continuity equation then reduces to

$$K(z) \frac{dn_j(z)}{dz} + \left[\frac{K(z)}{H} + w_d(z) \right] n_j(z) = -\Phi_j(z). \quad (7)$$

In § IV we shall apply equation (7) to the number density $n(z)$ of organic molecules or other chromophore particles for which the drift velocity can be neglected ($w_d \ll K/H$). Assume further that the particles are mainly produced at some higher level $z \approx Z_0 > 0$ and destroyed at some lower level $z \equiv 0$, so that the flux Φ equals the total production rate ($\text{cm}^{-2} \text{s}^{-1}$) for $0 \leq z \leq Z_0$ and $\Phi = 0$ outside that range. If the production level Z_0 is in the troposphere, the eddy diffusion coefficient is given by K_c in equation (3), which varies quite slowly over a scale height H . An approximate solution of equation (7), which neglects terms in dK_c/dz , is then

$$\begin{aligned} n(z) &\approx (\Phi H/K_c)[1 - \exp(-z/H)] \quad \text{for } 0 < z < Z_0, \\ &\approx (\Phi H/K_c) \exp[-(z - Z_0)/H] \quad \text{for } H \ll Z_0 < z. \end{aligned} \quad (8)$$

Thus particle number densities decline exponentially with altitude above the production level and decrease more slowly with depth below the production level. Mathematically, the solution in equation (8) depends on the boundary condition that $n(z) = 0$ for $z \leq 0$ and that Φ is already constant for infinitesimally small positive z . Physically, the requirement is merely that the destruction rate change from very small values (at positive z) to very large values (at negative z) over less than a scale height. This should be a good approximation since pyrolysis rates are very temperature-sensitive. (But note that the level $z = 0$ refers to different altitudes for different molecular species.)

The situation is more complicated if the production level Z_0 is in the mesosphere and the destruction level ($z \equiv 0$) in the troposphere, with $z = Z_p < Z_0$ representing the tropopause. However, neglecting again derivatives of $K = K_c$ (for $z < Z_p$) and assuming that $K = K_m$ (for $Z_p < z$) is proportional to $e^{z/H}$ as in equation (6), the continuity equation (7) can again be solved analytically. With the fact that $Z_p \gg H$ and $K_c(Z_p) \gg K_m(Z_p)$ for cases of practical interest, the solution can be approximated by

$$\begin{aligned} n(z) &\approx (\Phi H/K_c)[1 - \exp(-z/H)] \quad \text{for } 0 < z < Z_p, \\ &\approx \frac{\Phi}{K_m(z)} \left[z - Z_p + H \frac{K_m(Z_p)}{K_c(Z_p)} \right] \\ &\quad \text{for } Z_p < z < Z_0, \\ &\approx [\Phi(Z_0 - Z_p)/K_m(Z_0)] \exp[-(z - Z_0)/H] \\ &\quad \text{for } Z_0 < z. \quad (9) \end{aligned}$$

Thus particle number densities increase slowly with altitude above the destruction level until the tropopause, decline slower than exponentially ($\propto ze^{-z/H}$) between the tropopause and the production level, and decline exponentially above the production level. For mesospheric production and tropospheric destruction, we therefore expect maximum number densities just above the tropopause. Again, no particles exist at $z < 0$. Note that the mixing ratio ($\propto n/\rho_{\text{gas}}$) remains constant *above* the production level whether this level is in the mesosphere or troposphere. In reality, this mixing ratio would *decrease* slightly with increasing height z if some additional destruction takes place above the production level or if the drift velocity w_d is not entirely negligible.

III. THERMAL CONDENSATION IN DEEP CLOUD LAYERS

The thermal condensation of droplets to form cloud layers in the Jovian atmosphere has been discussed (Weidenschilling and Lewis 1973; Stauffer and Kiang 1974) only for the upper levels of the troposphere ($T \lesssim 300$ K), where direct observations are possible. Molecules involving H, C, N, O, P, and S have been considered, which lead especially to condensation of H_2O ($T \lesssim 275$ K), NH_4SH ($T \lesssim 220$ K), and NH_3 ($T \lesssim 160$ K). The condensation of droplets of more refractory materials in deeper layers (higher temperature, T) is also of some interest, especially for compounds containing Na and/or Cl. If such small grains or droplets can be convected to the upper troposphere, they can act as seed nuclei for the condensation of H_2O drops (at $T \approx 280$ K). Their abundance is also relevant for any hypothetical Jovian biology and for the question of the replication of terrestrial microbial contaminants in the Jovian clouds. The following crude estimates and conjectures should serve at least for purposes of orientation.

In the very deep interior of Jupiter where the density exceeds 0.2 gm cm^{-3} ($P > 10^5$ bar, $T \gtrsim 10^4$ K), in-

complete solubility of various substances in hydrogen could lead to substantial chemical separation. This possibility, discussed so far only for He (Salpeter 1973; Smoluchowski 1973), should be investigated further; however, we assume provisionally cosmic abundances of all elements (Allen 1973) at $P \approx 10^{3.5}$ bar ($T \approx 2500$ K), say. At this level practically all substances are gaseous. Refractory molecules begin to condense at slightly lower temperatures.

For each material, with f the cosmic abundance by number (mixing ratio) of the least abundant element in the compound, we must evaluate a number of quantities:

1. The equilibrium condensation temperature T_{con} appropriate to the Jovian troposphere, i.e., that temperature at which the saturation vapor pressure equals f times the pressure in equation (1). Values for T_{con} have already been given by Lewis (1969b).

2. Assuming the absence of any external seed nuclei, we calculate the amount of supercooling ΔT_{cr} required from homogeneous nucleation theory. For this purpose we need a parameter η , defined in equation (7) of Salpeter (1974), which is essentially the number of times appropriate molecules of a particular species stick to a given surface site on a droplet during a typical flow time. In that definition for η we use $s \approx 0.5$ for the surface sticking coefficient and equation (1) for the pressure, and replace the flow velocity v by the typical convection speed w_c in equation (3), which gives $\eta \approx f(T_{\text{con}}/175 \text{ K})^{4.2} \times 3 \times 10^{13}$. Values of f and T_{con} (taken from JANAF 1971) are given in Table 1 for a number of compounds, and η exceeds 4×10^8 in all cases. The ratio $\Delta T_{\text{cr}}/T_{\text{con}}$ is given by equation (9) of Salpeter (1974), but multiplied by a factor $6^{-1/2}$ (correcting an error kindly pointed out by B. Draine). This ratio is fairly small in the cases considered and not of direct importance for our crude estimates. But we do need the final radius a_f of typical drops which would result at the end of purely homogeneous nucleation.

At first sight one would expect a_f to be of order η times the intermolecular spacing in the liquid, but there are a number of correction factors. The most important correction is due to the fact that the drop radius a becomes large compared with the mean free path for a molecule in the gas, $l_m \approx (T/175 \text{ K})^{-2} \times 6 \times 10^{-5}$ cm. The droplet's growth is controlled by the diffusion speed rather than the gas-kinetic speed, and the rate is multiplied by a correction factor $(l_m/a) \ll 1$. Including some further logarithmic factors, we find, as a very rough approximation,

$$a_f \sim (175 \text{ K}/T)\eta^{1/2}(\log_{10} \eta)^{-3/4} \times 10^{-6} \text{ cm}. \quad (10)$$

Our values for a_f are given in Table 1 and have to be compared with a number of other length scales.

3. Let a_{Re} be a critical radius for a spherical droplet such that the hydrodynamic drag coefficient C_D is unity. For $a \ll a_{\text{Re}}$ the Reynolds number is small and the drag coefficient is given by the Stokes formula $C_D = (12\nu/aw_a)$, where w_a is the Stokes expression for the terminal vertical drift velocity of the sphere. Using

TABLE 1

EQUILIBRIUM CONDENSATION TEMPERATURE, T_{con} , AND ESTIMATES OF THE RELEVANT MIXING RATIO, f , THE RADIUS a_f , THE PARAMETER η_{vap} , AND THE MINIMUM MIXING RATIO f_m FOR A NUMBER OF SUBSTANCES ABOVE THEIR CONDENSATION LEVELS

Parameter	Fe	Mg ₂ SiO ₄	SiO ₂	Na ₂ Si ₂ O ₅	NaCl	NH ₄ Cl	(Na ₂ S)
$-\log_{10} f$	4.1	4.6	4.4	5.7	6.3	6.3	(5.7)
$T_{\text{con}}/100$ K.....	25	23	18	16	10	4	10
$a_f/10^{-3}$ cm.....	120	60	40	20	4	2	8
η_{vap}	60	20	2	1	0.1	0.03	0.4
$-\log_{10} f_m$	7.9	7.7	7.2	7.8	7.0	6.4	7.0

equation (1), we have

$$a_{\text{Re}} = 0.007 \text{ cm} \left(\frac{2}{\rho_{\text{dr}}} \frac{175 \text{ K}}{T} \right)^{1/3},$$

$$w_d(a) = \frac{2}{9} \frac{a^2 g \rho_{\text{dr}}}{\nu \rho_g}$$

$$\approx (0.15 \text{ cm s}^{-1}) \left(\frac{T}{175 \text{ K}} \right)^{-1/2} \left(\frac{\rho_{\text{dr}}}{2} \right) \left(\frac{a}{10^{-4} \text{ cm}} \right)^2, \quad (11)$$

where ρ_{dr} is the internal density (in gm cm⁻³) of a liquid drop. Another critical length is a_d , the droplet radius for which the drift velocity w_d equals the typical convection speed w_c in equation (3). For the cases of interest ($T \lesssim 2500$ K) we have $a_d < a_{\text{Re}}$, so that equation (11) holds. With $\rho_{\text{dr}} \approx 2$ and $\xi \approx 1$ in equation (3), we have

$$a_d \approx 0.002 \text{ cm} (T/175 \text{ K})^{-1/12}. \quad (12)$$

Large drops with $a \gg a_d$ "rain out" rapidly, whereas small droplets with $a \ll a_d$ are carried along by the convection pattern and can move up to higher levels.

For all cases in Table 1 (except possibly for NH₄Cl) we have $a_f > a_d$, so that homogeneous nucleation leads to large enough drops for most of the matter to be rained out. However, if a very large number of nucleation seeds are present originally, a large number of much smaller droplets condense out, and the droplets must grow before they can fall out as rain. Let a_{coa} be that radius for which $C_D = \rho_{\text{dr}}/\rho_g$:

$$a_{\text{coa}} \sim \left(\frac{\rho_{\text{dr}}}{2} \right)^{-2/3} \left(\frac{T}{175 \text{ K}} \right)^{1/3} \times 3 \times 10^{-4} \text{ cm}. \quad (13)$$

Once $a \geq a_{\text{coa}}$, droplets usually can grow very quickly by coalescence, but for $a < a_{\text{coa}}$ growth must occur by the slower process of smaller drops evaporating and the excess vapor diffusing to larger drops (Langmuir 1948; Mason 1972; Rossow 1976). An important parameter η_{vap} is the growth rate from this process (from radius $0.5a_{\text{coa}}$ to a_{coa} , say) expressed in units of H^2/K_c , a typical convection time. With an uncertainty of at least a factor of 10, we have

$$\eta_{\text{vap}} \sim 4 \times 10^4 f \left(\frac{T}{175} \right)^{7/6} \left(\frac{\rho_{\text{dr}}}{2} \right)^2. \quad (14)$$

If $\eta_{\text{vap}} \gg 1$ for a particular material, most of it will form into large "raindrops" in a cloud layer at levels close to the condensation temperature T_{con} , and only small amounts of the material will be found at higher, cooler levels. If $\eta_{\text{vap}} \ll 1$ one might expect only small droplets of the material to form, so that $w_d \ll w_c$ and upward convection can maintain an appreciable mixing ratio of the droplets at higher levels. In practice, however, various complications usually tend toward more rapid formation of larger droplets (Rossow 1976). For $\eta_{\text{vap}} \sim 10^{-1}$ or 10^{-2} , the circumstances are probably mixed: some rain near the T_{con} level, some small droplets a few scale heights higher up, but with a mixing ratio which decreases slightly with increasing height. Values for η_{vap} from equation (14) are given in Table 1. Except possibly for NH₄Cl, $\eta_{\text{vap}} \gg 10^{-2}$ as well as $a_f > a_d$, and most of the material rains out and cannot move up to higher levels. However, in upward-moving convection cells the saturation vapor pressure continues to fall; droplets then continue to condense out, but with decreasing values of the mixing ratio f and hence of the parameter η . Let f_m be that (decreased) value of the mixing ratio, for which the droplet size a_f (due to homogeneous nucleation) in equation (10) equals a_d . Values of f_m are also given in Table 1. The mixing ratio will not drop appreciably below f_m in upward moving convection cells, since droplets are now too small to rain out rapidly enough (and further growth of droplets is also too slow).

For the cases with $T_{\text{con}} \geq 1600$ K the radii satisfy $a_f > a_{\text{coa}}$, coalescence is rapid, and large drops are rained out immediately. At the high pressures in Jupiter's interior, liquid Mg₂SiO₄ (as well as Ca and Al silicates and metallic Fe) condenses before MgSiO₃ and before SiO₂. When liquid SiO₂ begins condensing near the 1800 K level, most of the metallic elements have already been rained out, but sodium has not. For pure Na₂SiO₅ our estimates indicate a slightly lower condensation temperature than for SiO₂, which introduces an uncertainty: It is conceivable that all the silicon has been rained out before sodium condenses, in which case gaseous NaCl and NaOH (since the elemental abundance of Na exceeds that of Cl) survive to higher, cooler levels. It is more likely that much of the sodium condenses out between 1800 K and 1600 K in the form of some sodium silicate-silica solution, in which case gaseous HCl and some NaCl survive to higher levels. In either case, more of the surviving NaCl condenses out near 1000 K; in the more likely

case, NH_4Cl condenses near 400 K; in the less likely case, Na_2S condenses near 1000 K.

We have some tentative implications for levels with $T \lesssim 700$ K, where Jovian biology (or at least organic chemistry) might be possible: Sodium (or other alkali metals and alkaline earths) and chlorine (or other halogens) cannot be present simultaneously. However, either sodium sulfide or (more likely) ammonium chloride is present. For the more likely case, some fraction of the NH_4Cl crystals are convected upward and act as seed nuclei for the condensation of water droplets, so that essentially no supercooling is present in the base level of the water clouds (Stauffer and Kiang 1974). For the less likely case of Na_2S crystals, convection over a larger height difference is required for nucleating the water, and f_m is slightly smaller. However, the chromophores to be discussed in § IV, as well as Na_2S and NH_4Cl , could probably also act as seed nuclei, and it seems generally safe to assume no supersaturation for water. We estimate below the amount of exogenous sodium which may arrive at the cloud level from micrometeoritic infall.

Since both sulfur and sodium have been detected in toroidal nebulae about Jupiter—probably arising from the surface of Io—these clouds are a potential source of S and Na in the clouds of Jupiter. From observations of forbidden S II circumjovian line emission, Brown (1976) calculates a total sulfur flux from the surface of Io of $10^{8.6 \pm 0.7} \text{ cm}^{-2} \text{ s}^{-1}$, equivalent to roughly $10^4 \text{ cm}^{-2} \text{ s}^{-1}$ at the Jovian clouds. This is some 8 orders of magnitude less than that expected from H_2S photodissociation (see § IV), and therefore is entirely negligible. The cosmic abundance of Na is at least an order of magnitude less than that of S, and so only very small quantities of sodium could be present at the Jovian clouds due to leakage from the Io Na toroid.

Approximate influxes of micrometeoritic sodium and sulfur, assuming the fluxes are the same on Jupiter as on Earth, and that micrometeorites are primarily cometary ices with cosmic abundances of other atoms, are $\sim 10^5 \text{ cm}^{-2} \text{ s}^{-1}$ for Na, and $\sim 10^6 \text{ cm}^{-2} \text{ s}^{-1}$ for S. Thus the micrometeoritic infall rate of these atoms is likely to exceed that from the Io-associated toroidal clouds. In the upper troposphere with $T \simeq 175$ K, equations (3) and (9) then give $n \sim 10^4$ Na atoms cm^{-3} , corresponding to a mixing ratio $f \lesssim 10^{-15}$, and even smaller at the water cloud levels. These values are small compared with the values of f_m in Table 1.

IV. PHOTOPRODUCTION OF MOLECULES AND CHROMOPHORES

a) Far-Ultraviolet

At thermal equilibrium methane is by far the most abundant carbon compound in the Jovian atmosphere, where it remains in gaseous form. Methane absorbs UV photons at all wavelengths shorter than 1600 Å, and the total flux of such photons at the top of the Jovian atmosphere (mainly from solar L_α at $\lambda = 1216$ Å) is $\sim 5 \times 10^9$ photons $\text{cm}^{-2} \text{ s}^{-1}$ (global diurnal average). Very little of the L_α photons are

scattered by neutral hydrogen (Carlson and Judge 1974), and about one-third of the photons process CH_4 into other hydrocarbons (Strobel 1973a, 1975). The dominant product is ethane with a predicted production rate of $R \sim 1 \times 10^9 \text{ C}_2\text{H}_6 \text{ cm}^{-2} \text{ s}^{-1} \sim 5 \times 10^{-14} \text{ gm cm}^{-2} \text{ s}^{-1}$. The ethane produced is rather stable and is destroyed mainly by eddy diffusion into the troposphere, followed by pyrolysis in deeper, hotter layers. For an assumed mesosphere eddy diffusion coefficient $K_m(z)$, accurate numerical calculations for the number density $n(z)$ of C_2H_6 can be carried out (Strobel 1975). However, equation (9) is sufficient for purposes of orientation (the largest uncertainty comes from uncertainties in K_m). Assuming the tropopause level Z_p to occur at $P \approx 0.5$ bar (with $P \sim 10^{-6}$ to 10^{-7} bar at the production level Z_0), and with $K_m(z)$ given by equation (6), the maximum ethane number density occurs one scale height H above the tropopause:

$$n_{\max} \approx \Phi H / K(Z_p + H) \\ \approx 5 \times 10^{12} \text{ cm}^{-3} \approx 5 \times 10^{-7} n_{\text{H}_2}, \quad (15)$$

where $K(Z_p + H)$ is the eddy diffusion coefficient evaluated at altitude $Z_p + H$.

The maximum value of the mixing ratio occurs just below the production level, and the total predicted column density N of ethane molecules is

$$N \approx \Phi H^2 / K_m(Z_p) \\ \approx 5 \times 10^{19} \text{ cm}^{-2} \approx 3 \times 10^{-3} \text{ g cm}^{-2}. \quad (16)$$

Ethane (and smaller amounts of acetylene) have indeed been detected in the Jovian mesosphere by means of the emission spectrum at $\lambda \approx 10 \mu\text{m}$ (Ridgway 1974). High-resolution spectra are not yet available, and the column density N of C_2H_6 from the present spectra depends strongly on the distribution of gas temperatures, which is not well determined by low-resolution spectra: If the temperature in the mesospheric inversion layer turns out to have a maximum value of 150 K, the observations indicate (Ridgway 1974) $\sim 0.02 \text{ g cm}^{-2}$ of ethane in this high-temperature region. This would be in very serious conflict with the predictions, since only a small fraction of the theoretical column density in equation (16) refers to the hotter region many scale heights above the tropopause. Presumably one is dealing with some combination of (a) higher mesospheric temperatures, (b) smaller diffusion rates than in equation (6), or (c) some additional source of ethane raising the production rate R above $10^9 \text{ cm}^{-2} \text{ s}^{-1}$.

Production rates from the same L_α radiation in the mesosphere for larger, more complex organic molecules have been estimated (Strobel 1975) to be factors of ~ 10 or 100 (by number) less than ethane, an estimate consistent with the data presented by Noyes and Leighton (1941), who remark that the ultraviolet irradiation of ethane leads to "a surprising variety of products," including unsaturated polymeric hydrocarbons. Assuming one-tenth the rate (by mass), the

mass-production rate R_{org} is $\sim 5 \times 10^{-15} \text{ g cm}^{-2} \text{ s}^{-1}$, and equation (16) would give a column density for complex organics of $N_{\text{org}} \sim 3 \times 10^{-4} \text{ g cm}^{-2}$.

Complex organic molecules may or may not be the mesospheric chromophores which have been inferred from the UV albedos: The measured albedo of Jupiter (Wallace *et al.* 1972; Savage and Caldwell 1974) to solar photons in the near-UV is quite low, with a minimum ~ 0.25 near $\lambda \approx 2800 \text{ \AA}$. Unit optical depth for pure (conservative) Rayleigh scattering by H_2 for 2800 \AA photons is reached at a level with $P \approx 0.3$ bar in the lower mesosphere. No simple molecules present near or above this level absorb in this wavelength region (NH_3 is effective only for $\lambda \lesssim 2300 \text{ \AA}$), and complex molecules or very small absorbing dust grains have been invoked to provide the absorption (Axel 1972). Absorption in this region can be provided by a range of not implausible organic molecules (Sagan 1968; Khare and Sagan 1973). A mass absorption coefficient near 2800 \AA of $\sim (2N_{\text{org}})^{-1} \sim 10^3 \text{ cm}^2 \text{ g}^{-1}$ would be required if organic molecules (beyond ethane) produced by α photons are responsible. This is within the range of measured absorption coefficients for complex organic molecules produced by ultraviolet light in crude Jupiter simulation experiments (see, e.g., Khare and Sagan 1973).

b) Cloud Models

The total thermal infrared flux emerging from Jupiter gives $T_{\text{eff}} \approx 127 \text{ K}$. Most of this flux emerges at wavelengths $\lambda \approx 20 \text{ }\mu\text{m}$ to $60 \text{ }\mu\text{m}$; the opacity source is mainly H_2 (with a small contribution from gaseous NH_3); and most of the radiation emanates from levels with $P \approx 0.7$ bar to 0.2 bar ($T \approx 150 \text{ K}$ to $\approx 115 \text{ K}$). Only a small fraction of the thermal flux emerges at wavelengths $\lambda < 15 \text{ }\mu\text{m}$, but the opacities of the main gaseous constituents of the Jovian atmosphere are low at some of these shorter infrared wavelengths. In the absence of any particulate matter (or complex molecules), radiation with $\lambda \approx 8.2 \text{ }\mu\text{m}$ to $9.5 \text{ }\mu\text{m}$ would emerge from levels with $T \approx 155 \text{ K}$, and radiation with $\lambda \approx 5 \text{ }\mu\text{m}$ from even deeper levels with temperatures up to $T \approx 300 \text{ K}$.

Assuming solar abundances of all elements in the Jovian interior and assuming thermochemical equilibrium, one can calculate condensation temperatures T_{con} for various species (cf. Lewis 1969a; Weidenschilling and Lewis 1973; Prinn and Owen 1976). T_{con} determines the level of each "cloud bottom," and above this level the gas-phase abundance is given by the saturation vapor pressure. The abundance and size distribution of droplets (or crystals) in the upper layers of a cloud cannot be calculated without detailed knowledge of the dynamics (see § III). The cloud bottoms for ice (and aqueous ammonia) are at levels with $T \approx 280 \text{ K}$, for NH_4SH at $T \approx 200 \text{ K}$, and for NH_3 at $T \approx 150 \text{ K}$ ($P \approx 0.7$ bar).

Measurements of spectral reflectivities for solar radiation in the visible range are now available separately for the bright zones and for the darker belts in the Jovian equatorial and temperate latitudes

(Orton 1975c). The fraction of the sunlight that is absorbed varies from only ~ 0.2 in zones to ~ 0.3 in belts for red light, but varies from ~ 0.3 in zones to ~ 0.5 in belts for blue light. The data at $\lambda \approx 20 \text{ }\mu\text{m}$ and $45 \text{ }\mu\text{m}$, separately for zones and belts (Orton 1975c), are compatible with a model which includes an optically opaque cloud top at the level ($T \approx 145 \text{ K}$, $P \approx 0.6$ bar) for zones, but not for belts. This model is not unique, but the postulated cloud top occurs close to the level at which solid NH_3 crystals are expected to precipitate out if the zones represent the upward draft in the overall circulation. The spectral data for $\lambda \approx 8$ to $14 \text{ }\mu\text{m}$ (averaged over some zones and belts), together with spatially resolved data at $\lambda = 8.11 \text{ }\mu\text{m}$ and $8.45 \text{ }\mu\text{m}$ (Orton 1975b), indicate the presence of some obscuring matter at altitudes above the $T = 150 \text{ K}$ level. The absorption spectrum of solid NH_3 crystals fits these data quite well, with more absorbing material over zones than over belts suggested by the data. Nevertheless, a small amount of absorption seems to be required over the belts as well, with an extent of only a few kilometers at levels with $T \approx 145 \text{ K}$ to 150 K indicated for this thin haze.

One question of primary concern is the nature and location of the red chromophores which are responsible for the absorption of visible sunlight over the belts (or at least for the preferential absorption in the blue). Upper limits to the location altitude can be inferred from the common observation that the red chromophores are sometimes overlain by time-variable white clouds. The relative heights are apparent because the interface between white and red material is frequently convex outward from the white clouds. As discussed, the highest lying clouds which are possible on Jupiter are ammonia cirrus clouds at levels with $T \approx 145$ to 150 K . The red chromophores must therefore reside mainly at deeper levels with $T > 145 \text{ K}$ and $P > 0.6$ bar. Emission at $\lambda \approx 5 \text{ }\mu\text{m}$ reveals infrared hotspots in only some regions of the belts (but in none of the zones) where the radiation emerges from deep levels with temperatures up to $T \approx 300 \text{ K}$. The red coloration is anticorrelated with these infrared hotspots (Keay *et al.* 1973; Westphal, Matthews, and Terrile 1974), which implies either that (a) the red chromophores reside above the level of some intermittent clouds which are opaque to $5 \text{ }\mu\text{m}$ radiation and which reside somewhere above the $T \approx 300 \text{ K}$ level; or (b) that the red chromophores are themselves intermittent and opaque at $5 \text{ }\mu\text{m}$. The infrared hotspots are associated with visually dark patches of bluish hue, probably connected with Rayleigh scattering rather than with blue chromophores, placing the blue regions at pressures of several bars, and $T \lesssim 280 \text{ K}$ (see Sagan 1971). To summarize: The red chromophores reside mainly in the troposphere ($T > 145 \text{ K}$), extending downward from the tropopause ($T \approx 145 \text{ K}$) to at most the $T \approx 300 \text{ K}$ level.

The condensation temperature of solid NH_3 is only slightly higher than the temperature ($T \approx 145 \text{ K}$) expected for the tropopause, so that the solid NH_3 clouds reside in the upper layers of the troposphere. The pattern of patches of white clouds overlying the

red chromophores changes on a time scale of a few weeks. This is comparable to the total tropospheric eddy diffusion time t_c in equation (3) if $\xi \approx 1$, but is also compatible with the longer total circulation time t_{cir} in Gierasch's model, since time scales for patches of horizontal extent $d_p \ll D_{\text{zb}}$ (the separation between zones and belts) are only of order $(d_p/D_{\text{zb}})t_{\text{cir}}$. The postulated intermittent $5 \mu\text{m}$ clouds underlying the red chromophores could in principle reside anywhere between the $T \approx 145 \text{ K}$ and $T \approx 300 \text{ K}$ levels, but on Gierasch's model these levels in belt regions represent a continuous downdraft of warming material which could not form NH_4SH or H_2O crystals. Solid NH_3 clouds can be present in belts to varying degrees, because the upper horizontal circulation path from zones to belts can include layers just below the tropopause which carry NH_3 crystals. On this picture the red coloration would have to be provided by red chromophores which more or less coexist with NH_3 clouds ($P \approx 0.5$ to 0.7 bar), but with varying amounts of (i) high-level clouds with small NH_3 crystals, (ii) red chromophores, and (iii) clouds at lower levels with larger NH_3 crystals.

c) Radiative Transfer Excursion

Besides the red chromophores we are also interested in inferred near-UV chromophores: The measured albedo of Jupiter (Wallace, Prather, and Belton 1974; Savage and Caldwell 1974) to solar photons in the near-UV ($\lambda \approx 2000 \text{ \AA}$ to 3500 \AA , say) is quite low, with a minimum albedo ~ 0.25 near $\lambda \approx 2800 \text{ \AA}$ (after rising slowly toward shorter λ , the albedo again seems to be lower for $\lambda < 2300 \text{ \AA}$). Absorption by H_2S , residing in the NH_4SH clouds at lower levels has also been considered (Prinn 1970, 1974; Lewis and Prinn 1970; Sagan and Khare 1971b; Lewis 1976). A computational problem is often presented by absorbers whose abundance decreases very rapidly with increasing altitude (because of condensation); we briefly review the relevant radiative transfer theory.

Consider plane-parallel geometry and assume that the scattering is isotropic. Let τ be the total extinction optical depth at some level (scattering plus absorption), $\bar{\omega}_0$ the single scattering albedo (ratio of scattering to extinction cross section) at the same level, and $\kappa \equiv [3(1 - \bar{\omega}_0)]^{1/2}$. If κ is independent of τ , the Eddington approximation is known even for slabs of finite thickness (Chandrasekhar 1960; Irvine 1975) and is discussed in our Appendix. The mean intensity $J(\tau)$ as a function of depth is particularly simple for a semi-infinite slab of constant κ (see eqs. [A3] to [A5] and eq. [A17]). Unfortunately, κ can be a very steep function of τ as in the example in Figure 2, which corresponds very roughly to absorption by H_2S and Rayleigh scattering by H_2 of 2500 \AA wavelength photons in the work by Prinn (1970). Prinn used equation (A3) for $J(\tau)$ in the integrand of an integral which evaluates the absorbed energy layer by layer. Unfortunately, this use of equation (A3) can lead to gross errors when κ is varying rapidly, and a more accurate numerical evaluation is given in our Appendix

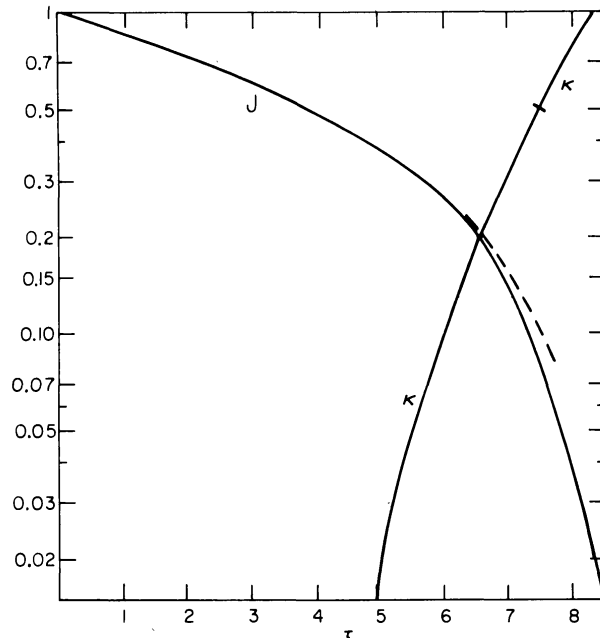


FIG. 2.—A model radiative transfer calculation for an assumed form of the parameter κ , as a function of total optical depth τ . Numerical results for the mean intensity J are given in the solid curve. The dashed curve is an analytic approximation, discussed in the text.

for the example in Figure 2. Fortunately, the correct result for the fraction f of the incident energy which is absorbed is fairly close to the following simple approximation, f_0 : Let τ_0 be the total optical depth at the level where κ equals some predetermined number, say $\kappa = 0.5$ (in our example $\tau_0 \approx 7.5$). Let f_0 be the fractional energy which would be absorbed according to the Eddington approximation if one had no absorption at all for $\tau < \tau_0$ and a perfect absorber at τ_0 . For diffuse incident illumination (instead of averaging over different angles of incidence) one has $f_0 = (0.75\tau_0 + 1)^{-1}$ if $\tau_0 \gg 1$ (see eq. [A16]). For the numerical example in the Appendix the value of f_0 corresponding to the choice $\kappa = 0.5$ for τ_0 fits the correct f quite well.

d) Near-Ultraviolet

Solar photons in the near-UV ($\lambda \approx 2000 \text{ \AA}$ to 3000 \AA , say) are much more abundant than $L\alpha$ photons. It is of interest to speculate about materials which absorb in the near-UV to see (i) if their absorption can explain the low observed albedo in the near-UV, and/or (ii) if the end products of reactions initiated by such absorption can provide the red chromophores for the troposphere, and (iii) how much complex organic material can be so produced.

The absorption of solar radiation with $\lambda \approx 2300 \text{ \AA}$ to 2700 \AA by H_2S in the upper layers of the troposphere has been discussed by the authors listed above (for $\lambda > 2700 \text{ \AA}$ the absorption by H_2S is too weak and photons with $\lambda < 2300 \text{ \AA}$ are already absorbed by NH_3 at higher altitudes). The total flux in this wavelength range (diurnal mean) is about 1×10^{13} photons

$\text{cm}^{-2} \text{s}^{-1}$, and some fraction f_s of these photons are absorbed by H_2S . We first present estimates if an *ad hoc* value of $f_s = 0.1$ is assumed (and $\xi = 1$ in eq. [3]).

Laboratory simulation experiments by near-ultraviolet irradiation of CH_4 , C_2H_6 , NH_3 , H_2O , and H_2S mixtures at ~ 1 bar pressures have been performed, but without initial excess hydrogen (Sagan 1971; Sagan and Khare 1971*a, b*; Khare and Sagan 1973, 1975). Hydrogen sulfide is the primary photon acceptor in these experiments. Amino acids were produced in these experiments with a quantum yield of $\sim 10^{-4}$ for molecular weights ~ 100 ($\sim 10^{-2}$ amu photon $^{-1}$). The quantum yield of all organics in such experiments is of the order of 100 times larger (of the order of 1 amu photon $^{-1}$). Some red chromophores were abundantly produced, consisting mainly of polymeric sulfur, but including a substantial fraction of organic compounds. The overall mass absorption coefficient for blue light of these chromophores is $k \sim 10^3 \text{ cm}^2 \text{ g}^{-1}$. If such particles are produced in Jupiter at the rate of one S-bond per absorbed photon ($R \sim 10^{12} \text{ S cm}^{-2} \text{ s}^{-1} \sim 5 \times 10^{-11} \text{ g cm}^{-2} \text{ s}^{-1}$), their column density, N , over a few scale heights down to the thick water clouds, is needed. According to equations (3) and (8), $N \approx 2RH^2/K_c \sim 10^{-4.5} \text{ g cm}^{-2}$ and the optical depth to absorption in the blue is $\tau = kN \sim 0.03$. This is almost two orders of magnitude smaller than the observed optical depth. Moreover, the reaction of eight sulphydryl radicals to form S_8 is poisoned by competing reactions, and the S_8 quantum yield must be significantly less than 1.

In the laboratory experiments cited, organic molecules, but not polymeric sulfur, were produced from superthermal hydrogen atoms. In the presence of a thousand times more H_2 (by number), the quantum yield might be expected to decrease by about the same factor, if energy loss of the fast atoms is mainly by elastic collisions, to $\sim 10^{-3}$ amu photon $^{-1}$. The total production rate would then be quite small, $R \sim 5 \times 10^{-14} \text{ g cm}^{-2} \text{ s}^{-1}$ (which is still 10 times larger than our estimated R_{org} for the mesosphere). The corresponding optical depth for organic chromophores is, then, many orders of magnitude below the observed value. Many uncertainties remain, however, including indirect effects of scattering. In the laboratory experiments cited, large quantities of molecular hydrogen are produced during the irradiation because the end products are unsaturated, and it may be that the correction factor from laboratory to Jovian situation is closer to 10^{-2} than to 10^{-3} . It is also possible that somewhat longer wavelength ultraviolet light—perhaps as long as 2900 Å—is still effective in these syntheses. Recent experiments (Ferris and Chen 1975) have shown that 1849 Å irradiation of mixtures of CH_4 and NH_3 in a 10:1 excess of H_2 produce a variety of organic molecules in very high yields, presumably by the generation of hot hydrogen atoms from ammonia photodissociation. These results suggest that the effects of H_2 dilution on poisoning organic photochemistry may be slower than linear. Hence the contribution of organic polymers to near-UV photoproduct optical frequency absorbers on Jupiter may be significant.

Polymeric sulfur is not produced by hot hydrogen atoms in such experiments, and so the scaling from laboratory to Jupiter is more direct in this case. However, even here, and even under the excessively optimistic assumption that every H_2S photodissociation event leads to polymeric S, the implied optical depth falls short by two orders of magnitude from matching the observed values; moreover, pure polymeric sulfur fits the observed optical properties of the Jovian red chromophores poorly at best (Rages and Sagan, in preparation).

We have seen that a slow, deep circulation pattern is likely to extend all the way from the tropopause down to the level with $T \approx 300 \text{ K}$ (Gierasch 1976) with $\xi \sim 0.01$ in equation (3). Abundances of reaction products are proportional to ξ^{-1} and also to $(f_s/0.1)$, which was claimed to be as large as 4 by Prinn (1970). One might then expect H_2S photolysis to dominate chromophore production, but this still seems unlikely for three reasons: (1) As discussed in § IVc and in our Appendix, Prinn's (1970) estimate of $f_s \approx 0.4$ is likely to be an overestimate since $f_0 \equiv (0.75\tau_0 + 1)^{-1}$ is smaller. Thus $f_s \leq 0.2$ is more likely even in the absence of any scatterers (other than H_2) or other absorbers above the H_2S levels. The smallness of f_s is also suggested by the fact that the observed albedo of Jupiter does *not* increase from $\lambda \approx 2800 \text{ Å}$ (where H_2S is ineffective) to $\lambda \approx 2600 \text{ Å}$ (where H_2S absorption should already be strong). (2) Since H_2S cannot itself be the cause for the low albedo in this wavelength range, whatever absorbers are the cause must lower f_s further. (3) Most important, the systematic deep circulation pattern mentioned before depresses H_2S photolysis *both* in zones and belts: In the updraft, represented by zones, H_2S is abundant in the NH_4SH clouds, but NH_3 clouds are *above* these layers and prevent most of the solar radiation from penetrating down. In the downdraft, represented by belts, the NH_3 clouds are absent (or at least diminished), but the material moving downward is practically devoid of H_2O and H_2S (which condensed out on the previous upward journey). H_2O and H_2S are again abundant in deep levels with $T \gtrsim 300 \text{ K}$, but little of the near-UV penetrates to such depths.

NH_3 absorbs solar photons of wavelength $\lambda < 2300 \text{ Å}$, which are somewhat less abundant than photons between 2300 Å and 2700 Å. On the other hand, NH_3 should not suffer the shielding difficulties experienced by H_2S because it resides in the *highest* cloud layer which extends up to the tropopause. NH_3 should therefore be abundant in both zones and belts and even flows into the lower mesosphere at a non-negligible rate. It is therefore likely that most of the photons with $\lambda \approx 2300 \text{ Å}$ are absorbed by ammonia (Strobel 1973*b*), which is compatible with the observed decline in albedo from $\lambda > 2300 \text{ Å}$ to $\lambda < 2300 \text{ Å}$. Hydrazine particles are also produced by ammonia photolysis and may provide a suitable explanation for the low albedo near $\lambda \approx 2800 \text{ Å}$ (Prinn 1974). Moreover, organic molecules produced by NH_3 photodissociation at $\lambda < 2300 \text{ Å}$ could conceivably be the principal source of red chromophores, if the quantum

yields of such reactions with $10^3:1$ H_2 dilutions are as high as the experiments of Ferris and Chen (1975) suggest.

e) Optical Frequency Photoproduction of Chromophores

We here consider two possibilities: If the circulation in the upper part of the troposphere is as slow as Gierasch (1976) suggests, then $\xi \lesssim 0.01$ in equation (3) and column densities obtained from equation (8) are increased by two orders of magnitude; thus polymeric sulfur or complex organics might provide the red chromophores. But, as we have seen, there are other problems with the contention that the chromophores are produced by H_2S photolysis. These problems are avoided if shorter wavelength photolysis of NH_3 is an adequate source of complex organic chromophores, but this is a questionable proposition considering the lower photon flux at $\lambda < 2300 \text{ \AA}$, and whatever is the correct value of the poisoning of organic photochemical synthesis in a $10^3:1$ H_2 dilution. If, on the other hand, ξ turns out to be of order unity, then ultraviolet photochemistry cannot in any case provide the observed chromophores at a sufficient rate. Thus in both cases we are led to the possibility that photochemistry at optical frequencies, where more total energy is available, is involved in chromophore production. But no chemical bonds of even moderately abundant molecules can be broken by photons of wavelengths longer than 3500 \AA on Jupiter, from which it follows that optical frequency photochemistry must be at least a two-photon process. However, such processes appear to be exclusively biological. We therefore find ourselves led unexpectedly to the hypothesis that the Jovian chromophores are biological in origin and that there is an abundant biota in the Jovian clouds.

Let us assume that the optical chromophores are contained primarily within Jovian organisms in the upper troposphere—organisms driven by visible light photosynthesis, perhaps primarily in the blue, and utilizing the abundant methane, water, and ammonia. Terrestrial algae (using CO_2 instead of CH_4) under laboratory conditions (Lehninger 1972) have a quantum yield for synthesizing glucose of about $4 \text{ amu photon}^{-1}$ (in the visible). The equivalent maximum production rate of biological material in the Jovian troposphere would be about $R = 3 \times 10^{-9} \text{ g cm}^{-2} \text{ s}^{-1}$. With a mass absorption coefficient of $k \approx 10^3 \text{ cm}^2 \text{ g}^{-1}$, such organisms would yield an optical depth of $\tau \approx 2$, slightly more than required by the observations. If the parameter ξ turns out to be of order 10^{-2} , and the red chromophores are due to Jovian photosynthetic organisms, R and/or K would have to be smaller.

Thus Jovian organisms having metabolic and photosynthetic parameters typical of terrestrial algae are able to account for the optical chromophores on Jupiter. Such organisms must, however, be adapted to the Jovian environment, and in particular must maintain a steady-state population in the face of convective pyrolysis. Likely ecological niches for such

organisms, as determined by the hydrodynamics on Jupiter, are discussed in the following sections. The following discussion can, however, be treated independently of the hypothesis that Jovian chromophores are biogenic.

V. SINKERS AND FLOATERS

If there is a Jovian biology, we would expect it to fill a rich variety of ecological niches. The best terrestrial analogy seems to be the surface of the sea. Oceanic phytoplankton inhabit a euphotic zone near the ocean surface where photosynthesis is possible. They are slightly denser than seawater and passively sink out of the euphotic zone and die. But such organisms reproduce as they sink, return some daughter cells to the euphotic zone through turbulent mixing, and in this way maintain a steady-state population. (The early stages of sinking move the phytoplankton from a region of depleted resources into a region of abundant nutrients, thus stimulating replication.)

A more elaborate adaptation is provided by fish and other organisms with float bladders which use metabolic energy to maintain a habitat at suitable pressure levels. They are generally not photosynthetic autotrophs, but rather heterotrophs living on organic molecules produced by autotrophs. A third ecological niche is filled by marine predators, one step further up the food chain, which hunt heterotrophs.

In the following discussion we will consider three comparable ecological niches on Jupiter: The primary photosynthetic autotrophs, which must replicate before they are pyrolyzed, will be described as sinkers. A second category of larger organism, which may be either autotrophs or heterotrophs but which actively maintain their pressure level, will be described as floaters. A third category of organisms actively seek out other organisms; we call these hunters, although, as we shall see, the distinction between hunting and mating under these conditions is not sharp. Finally, there is a category of organisms which live almost at pyrolytic depth. They are scavengers, metabolizing the products of thermal degradation of other organisms. For our purposes, these pyrolytic scavengers are identical with floaters. In the following two sections we estimate the growth time t_{gr} required for an organism to double its mass.

We first consider passive organisms with positive excess density $\Delta\rho_a$ above the gas density ρ_g . Such organisms falling under gravity through the atmosphere rapidly acquire a vertical drift velocity, w_d , which depends on the location and size of the organism and increases with increasing $\Delta\rho_a$. There is a premium on keeping $\Delta\rho_a$ and hence w_d small, and we consider only organisms in the shape of thin, gas-filled balloons. Such organisms have been briefly proposed before, both for Jupiter (Shklovskii and Sagan 1966) and for Venus (Morowitz and Sagan 1967).

For simplicity we treat a spherical shell of outer radius a and skin thickness $d \ll a$. In general we consider organisms filled with gas of the same temperature

and mean molecular weight (2.2) as the surrounding ambient atmosphere. The lack of buoyancy is then controlled by the excess averaged density due to the skin, $\Delta\rho_a = (3d/a)\rho_g$, where we assume the biological skin material to have unit density (1 g cm^{-3}).

For sufficiently small radius a of an organism, the Stokes formula in equation (11) holds (with $\rho_{\text{air}} \rightarrow 3d/a$) for the drift velocity w_d and the drag coefficient $C_D \approx 12\nu/aw_d$ is large. Let a_{Re} be a critical radius for which this relation gives $C_D = 1$ (Reynolds number = 24), so that

$$w_d = \frac{2}{3} \frac{gad}{\nu\rho_g} \quad \text{for } a \ll a_{\text{Re}},$$

$$a_{\text{Re}} \equiv (6\nu^2\rho_g/gd)^{1/2}. \quad (17)$$

For large organisms with $a \gg a_{\text{Re}}$ (large Reynolds number), the flow around the body becomes turbulent and the drag coefficient C_D (\equiv drag force/ $0.5\pi a^2\rho_g w^2$) is close to 0.5 (see, e.g., Batchelor 1970). In this regime

$$w_d \approx 4(gd/\rho_g)^{1/2}. \quad (18)$$

We shall have to consider separately organisms living below and above the tropopause. The troposphere provides conditions closest to terrestrial ones (similar temperatures and abundant water in liquid or vapor form). We assume that the organisms can survive there over a range L of vertical height ($L \approx 5H$, say), centered approximately on the level with $T \approx 300 \text{ K}$. An important time scale is then a nominal drift time $t_d \equiv L/w_d$. We consider the skin thickness d as an unknown parameter, with $d \sim 10^{-4} \text{ cm}$ possibly a typical value (biological unit membranes on Earth have $d < 10^{-5} \text{ cm}$, but mechanical strength is required for the skin). Using equations (1) and (11) and evaluating coefficients at the level with $T = 300 \text{ K}$, we find

$$t_d \approx \frac{L}{5H} \left(\frac{T}{300 \text{ K}} \right)^{1.5} \frac{1 \text{ cm } 10^{-4} \text{ cm}}{a} \frac{10^{-4} \text{ cm}}{d} 1.3 \times 10^4 \text{ s}$$

for

$$a < a_{\text{Re}} \approx \left(\frac{10^{-4} \text{ cm } 300 \text{ K}}{d} \frac{300 \text{ K}}{T} \right)^{1/2} 0.039 \text{ cm}. \quad (19)$$

For $a > a_{\text{Re}}$, on the other hand, equation (18) gives a drift time which depends on d but not directly on radius a ,

$$t_d \approx \frac{L}{5H} \left(\frac{T}{300 \text{ K}} \right)^2 \left(\frac{10^{-4} \text{ cm}}{d} \right)^{1/2} 2.5 \times 10^5 \text{ s}. \quad (20)$$

The eddy diffusion coefficient K_c in the convective troposphere is fairly large, and we also have to consider the contribution of eddy diffusion to the organism's downward motion over a vertical distance L . We are interested in cases where L is larger than H and the effective circulation time t_{cir} for downward diffusion is then not given by L^2/K_c : With $L \gg H$ and K_c a slowly varying function of height, the first

derivative term in equation (7) can be neglected and eddy diffusion has the same effect as increasing w_d to $(w_d + H^{-1}K)$. The relevant time scale is then linear in L and is approximated by the smaller of t_d and the quantity

$$t_{\text{cir}} = \frac{L}{H} t_c = \frac{LH}{K_c} \approx \frac{L}{5H} \left(\frac{T}{300 \text{ K}} \right)^{5/3} 3.7 \times 10^6 \text{ s}, \quad (21)$$

where we have used equation (3) and assumed $\xi \approx 1$. If $d \approx 10^{-4} \text{ cm}$, then eddy diffusion competes with gravitational fall only for microorganisms with $a \lesssim 30 \mu\text{m}$. Thus Jovian organisms the size of small terrestrial protozoa and prokaryotes have typical times for falling through the troposphere to pyrolytic depths of 1 to 2 months. To maintain a steady-state population, they must only replicate in that time scale.

In the Jovian mesosphere the temperature is low (we assume $T \approx 150 \text{ K}$) and water is absent, but some biologies have nevertheless been envisioned for such environments (see, e.g., Pimentel *et al.* 1966; Sagan 1970). We shall see that the lower, denser layers of the mesosphere are the most advantageous for the growth of such organisms; eddy diffusion is negligibly slow here compared with the downward drift velocity w_d . For organisms operating between a lower pressure P and the tropopause (pressure $\sim 1 \text{ bar}$), the drift-time L/w_d becomes

$$t_d \approx \ln \left(\frac{1 \text{ bar}}{P} \right) \frac{1 \text{ cm } 10^{-4} \text{ cm}}{a} \frac{10^{-4} \text{ cm}}{d} \times 930 \text{ s}$$

for

$$a < a_{\text{Re}} \approx \left(\frac{10^{-4} \text{ cm } 1 \text{ bar}}{d} \frac{1 \text{ bar}}{P} \right)^{1/2} 0.044 \text{ cm}. \quad (22)$$

For larger organisms, $a > a_{\text{Re}}$, the expression for large Reynolds number gives

$$t_d \approx \ln \left(\frac{1 \text{ bar}}{P} \right) \left(\frac{10^{-4} \text{ cm } P}{d} \frac{P}{1 \text{ bar}} \right)^{1/2} 1.6 \times 10^4 \text{ s}. \quad (23)$$

To obtain the pyrolysis time scale this number must be added to the appropriate tropospheric time scale given by equations (19), (20), and (21).

The expressions given above for t_d hold only for balloon organisms with ambient atmosphere inside. For organisms capable of pumping gas, buoyancy can be achieved while maintaining pressure equilibrium by keeping the interior gas pure hydrogen with molecular weight $\mu = 2.0$ instead of the ambient hydrogen-helium mixture with $\mu = 2.2$. A pumped organism can thus float if $\Delta\rho_a = (3d/a)\rho_g < 0.1\rho_g$. This requires radii a larger than a threshold radius a_{fl} for floating, given by

$$a_{\text{fl}} \approx \left(\frac{d}{10^{-4} \text{ cm}} \right) \left(\frac{T}{150 \text{ K}} \right) \left(\frac{1 \text{ bar}}{P} \right) \times 16 \text{ cm}. \quad (24)$$

Instead of maintaining a hydrogen interior, an organism could use a fraction of its metabolic energy release to heat its interior gas. The temperature difference ΔT between interior and exterior is determined by the metabolic rate and the thermal diffusion coefficient of the gas. Except at very high pressures, the thermal diffusion is fast enough to keep $\Delta T/T \ll 0.1$, so that smaller values of $\Delta\rho_a$ and larger radii than a_{fl} are required. Buoyancy from a hot interior is thus likely to be less advantageous than pumping out helium. Note that Jovian floaters are macroscopic organisms (eq. [24]). Specialized floaters, with a range of organ systems, might have an effective value of $d \sim 1$ cm as terrestrial reptiles and mammals do; in that case, floaters would have kilometer dimensions, a size within the resolution capability of the *Mariner Jupiter/Saturn* flyby imaging system. The existence of very large floaters is, however, limited by metabolic constraints described in the next section.

VI. GROWTH OF PASSIVE SINKERS AND FLOATERS

We defer for the moment further questions of buoyancy and of powered locomotion, and consider a range of metabolic niches. Organisms—sinkers or floaters—may be photosynthetic autotrophs, obtaining their free energy directly from sunlight. They may also be heterotrophs, of which we distinguish two classes: (i) those which feed on organic molecules of non-biological origin (e.g., ethane, an ultraviolet photoproduct), which reach the organism by molecular diffusion; and (ii) those which feed on organic matter in smaller organisms or their fragments which reach the larger organism because of the difference in vertical drift velocity w_d between predator and prey. Active hunters described in the following section are a related subclass. In all cases we must estimate the growth time $t_{gr} \equiv [2d \ln a/dt]^{-1}$ and compare it with the drift time t_d (or with t_{cir} if that should be smaller). We shall see that the ratio t_{gr}/t_d increases with the radius a of the organism; we are interested in the maximum radius a_{max} for which this ratio is unity. If a_{max} is appreciably larger than the minimum size a_{min} for a particular life style, then a biology can be maintained by an organism fragmenting into many smaller organisms or dispersules *before* it reaches size a_{max} , i.e., before it has drifted downward to a pyrolytic death. If $t_d \gg t_{cir}$ for the dispersules, they can be circulated upward, grow to a_{max} , and complete the life cycle.

We saw in § IV that the most favorable region for direct photosynthesis is probably the upper troposphere, just above the water clouds (with $T \approx 300$ K, $P \approx 5$ bar). Methane, ammonia, and water building blocks are abundantly available there to a photosynthesizing organism, and the growth rate is controlled by the deposition of free energy from solar photons. Furthermore, the observed optical chromophores can be explained by such organisms at such a level. We saw that a value for the production rate of $R \approx 3 \times 10^{-9}$ g cm $^{-2}$ s $^{-1}$ seems reasonable, and we

find for the growth time

$$t_{gr} \equiv \frac{a/2}{da/dt} = \frac{4d}{R} = \frac{d}{10^{-4} \text{ cm}} \frac{3 \times 10^{-9}}{R} 1.3 \times 10^5 \text{ s.} \quad (25)$$

Equating this time with t_d in equation (19) then gives for a_{max} , the maximum radius to which an organism can grow,

$$a_{max} \approx (10^{-4} \text{ cm}/d)^{2/3} 0.1 \text{ cm.} \quad (26)$$

Values of $a_{min} \lesssim 10^{-3}$ seem perfectly feasible, so that one organism can produce more than 10^4 dispersules for which $t_d \ll 4 \times 10^6 \text{ s} \approx t_{cir}$. The steady-state population of such organisms would then be controlled only by competition for sunlight, and not by gravitational fallout to pyrolytic depths.

Consider next the diffusion onto the skin of an organism of some organic molecule with molecular weight μ and abundance in the surrounding atmosphere of ρ_0 (in g cm $^{-3}$ of atmosphere). Ethane is the lowest mass ($\mu = 30$) organic molecule which carries free energy (relative to methane, the prevalent carbon molecule at thermal equilibrium). The diffusion coefficient D of ethane in the Jovian H-He mixture is about 0.4 times the viscosity ν of this mixture (Strobel 1973), and for heavier molecules D scales reciprocally as the cross section of the molecule. For approximately spherical organic molecules we adopt

$$D \approx 0.4\nu(\mu/30)^{-2/3}, \quad (27)$$

with ν given by equation (11). If $\nu > D \gtrsim (aw_d/12)$, the diffusion is almost independent of the motion of the sphere, and the steady-state rate for diffusion onto the surface is $4\pi a^2(\rho_0 D/a)$. Let ϵ be the ratio of increased body mass of the organism to the mass of ingested metabolites. Assuming unit density for the skin material, the growth time is then

$$t_{gr} = ad/2\epsilon\rho_0 D. \quad (28)$$

At a mesospheric level with pressure P (in bars), for molecules produced at a mass rate of $R = \mu\Phi$ at some *higher* level, equations (6) and (9) give $\rho_0 \approx (\mu\Phi H/100)P \ln P^{-1}$. The growth time in the mesosphere is then

$$t_{gr} \approx \frac{a}{1 \text{ cm}} \frac{d}{10^{-4} \text{ cm}} \frac{(\mu/30)^{2/3}}{\ln(1 \text{ bar}/P)} \times \left(\frac{5 \times 10^{-14}}{\Phi} \right) \frac{0.03}{\epsilon} 1.8 \times 10^6 \text{ s.} \quad (29)$$

For ethane an efficiency factor $\epsilon \sim 0.03$ seems reasonable and $R \sim 5 \times 10^{-14}$ g cm $^{-2}$ s $^{-1}$ has already been discussed; for UV photoproduction of more complex organic molecules we may leave $\epsilon \sim 0.3$ and $R \sim 5 \times 10^{-15}$ gm cm $^{-2}$ s $^{-1}$, so that $R\epsilon$ is the same, but the factor $\mu^{2/3}$ makes heavier molecules less favorable. Replacing the slowly varying factor $\ln(1/P)$ by 3 and

$R\epsilon$ by 1.5×10^{-15} , we find from equations (22) and (29),

$$a_{\max} \sim (10^{-4} \text{ cm}/d)(\mu/30)^{-1/3} \times 0.07 \text{ cm}. \quad (30)$$

If $\Phi\epsilon$ is particularly large and/or d particularly small, an organism can grow beyond size a_{Re} , and the diffusion rate now depends on the drift speed w_d , given by equation (18). We omit the complicated transition region $a \approx a_{\text{Re}}$ and make only order-of-magnitude estimates: There is a boundary layer in the flow around the sphere of thickness $b \approx a(4\nu/aw_d)^{1/2} \ll a$, such that the flow speed a normal distance y from the body is $\sim (y/2b)w_d$. With $D < \nu$ the typical stand-off distance for diffusion onto the body surface is $b_D \approx 2b(D/\nu)^{1/3}$ and the diffusion rate is $\sim 4\pi a^2(\rho_0 D/b_D)$, so that

$$t_{\text{gr}} \sim (2d/\epsilon\rho_0)(a/Dw_d)^{1/2}(\nu/D)^{1/6}. \quad (31)$$

For the mesosphere this gives

$$t_{\text{gr}} \sim \left(\frac{a}{1 \text{ cm}}\right)^{1/2} \left(\frac{d}{10^{-4} \text{ cm}}\right)^{3/4} \left(\frac{1 \text{ bar}}{P}\right)^{1/4} \frac{(\mu/30)^{4/9}}{\ln(1/P)} \\ \times \left(\frac{5 \times 10^{-14} \cdot 0.03}{\Phi \epsilon}\right) 8 \times 10^4 \text{ s}. \quad (32)$$

The same basic formulae apply in the troposphere, but ρ_0 is now much smaller for the same value of Φ because of the larger eddy diffusion coefficient, K_c . On the other hand, we have seen that photosynthesis may be going on there, and this may release complex organic molecules at a faster rate Φ . Substituting $\rho_0 = RH/K_c$ and using equation (3), we find (for $a < a_{\text{Re}}$)

$$t_{\text{gr}} \approx \frac{a}{1 \text{ cm}} \frac{d}{10^{-4} \text{ cm}} \left(\frac{T}{300 \text{ K}} \frac{\mu}{30}\right)^{2/3} \\ \times \left(\frac{3 \times 10^{-9} \cdot 0.3}{\Phi \epsilon}\right) 8 \times 10^7 \text{ s}. \quad (33)$$

Comparison with equation (19) shows a_{\max} to be of order $(10^{-4} \text{ cm}/d)(30/\mu)^{1/3} 0.013 \text{ cm}$, which is just macroscopic.

If small tropospheric photosynthetic organisms have radii $a_s \ll 0.01 \text{ cm}$, their drift speeds are even smaller than the eddy circulation speed and their abundance is still given by $\rho_0 = RH/K_c$. A larger organism of radius a , drifting downward with speed w_d , can grow by coalescing with such small organisms if the encounter satisfies certain conditions. These conditions are similar to those governing the coalescence of raindrops (Mason 1972; Rossow 1976). In analogy with equation (13) one finds, independent of a_s , and provided $d \ll a_s < a$, the requirement that $a > (10^{-4} \text{ cm}/d)(T/300 \text{ K}) 0.002 \text{ cm}$. If these conditions are satisfied, the larger organisms incorporate mass from the smaller ones at a rate of $4\pi a^2 w_d \rho_0$, so that $t_{\text{gr}} \approx$

$(4d/R)(K_c/Hw_d)$. If $a \gtrsim a_{\text{Re}} \sim 0.04 \text{ cm}$, then

$$t_{\text{gr}} \sim \left(\frac{d}{10^{-4} \text{ cm}}\right)^{1/2} \left(\frac{T}{300}\right)^{1/3} \left(\frac{3 \times 10^{-9} \cdot 0.3}{\Phi \epsilon}\right) \\ \times 2.5 \times 10^4 \text{ s}. \quad (34)$$

Neither t_{gr} nor t_d in equation (20) depends explicitly on radius a . An organism can then grow indefinitely as long as $(d/10^{-4} \text{ cm}) \lesssim (T/300 \text{ K})^{5/3}$.

Thus, provided the membrane thickness stays smaller than about $1 \mu\text{m}$, such passive sinkers can grow by coalescence with smaller organisms to sizes larger than a_{fl} as given by equation (24). This provides one evolutionary pathway from sinkers to floaters. However, the condition on membrane thickness is very restrictive. Floaters of this sort are unlikely to be much more stable than soap bubbles, and the organ systems which large organisms require could not be accommodated with the thin skin thickness. However, as we shall see in the following section, the hunting lifestyle provides a way out of this dilemma.

To summarize the situation so far: Sinkers can grow and produce reproductive dispersules in a stable, steady-state life cycle if they either (a) are mesospheric heterotrophs or photoautotrophs, or (b) are tropospheric photoautotrophs. Passive floaters exist only if (1) their skin can be made particularly thin, and (2) a significant fraction of the smaller photoautotrophs are available as food.

VII. POWERED LOCOMOTION AND COALESCENCE

We saw that the efficiency of utilization of metabolites diffusing onto the surface of a freely falling organism decreases with increasing mass of the molecule. However, for even more massive metabolites and organisms approaching each other with some relative drift velocity, growth by coalescence is again moderately efficient. The growth rate by coalescence can be increased greatly if organisms are capable of powered locomotion and can steer toward each other. We shall not discuss the predator-prey relationships of a strict hunting doctrine, but rather only an ecology in which an organism approaches another, coalesces into one larger organism which approaches other organisms, etc. It is clear that this hierarchical mating doctrine can also serve the traditional terrestrial function of mating, namely, the exchange of genetic material. A strict hunting doctrine in which one of the partners in such a coalescence is noncooperative will be less efficient than the doctrine discussed here. For convenience, however, we will describe both doctrines as hunting. In the following discussion we will assume that only one partner in such a mating event is active in the search; for this reason mating, hunting prey, and hunting abiological organic molecules are not extremely different. The doctrine in which both organisms are active in seeking partners would be more efficient than the ones described below.

For simplicity we assume the presence, with number density n , of organisms with radii of order a_1 at some upper injection level $z = Z_1$. The organisms coalesce

and grow as they drift downward, so that the size distribution changes with height z . Let $n(a, z)$ and $\rho(a, z) = (4\pi a^2 d)n(a, z)$ be their steady-state number density and mass density, respectively, per logarithmic interval of radius a . In principle we have a relation like equation (7) separately for each value of a , with the right-hand side representing the flux from one size range to another. We shall make only order-of-magnitude estimates for $\bar{a}(z)$, the mean radius of organisms at level z , and for $n(z) \equiv \int d \ln an(a, z)$.

We assume that the organisms are sufficiently large that $w_d(z)$, the drift velocity for radius $\bar{a}(z)$ at height z , is much larger than K/H in equation (7). Multiplying by mass (assuming as usual unit density for the skin material) and integrating over sizes, we find

$$[4\pi a^{-2}(z)d]w_d(z)n(z) = \epsilon(z)R. \quad (35)$$

In this relation R is the constant rate in $\text{g cm}^{-2} \text{s}^{-1}$ at which mass in the form of organisms enters the upper level $z = Z_1$; $\epsilon(z)$ is a slowly varying factor (slightly smaller than unity) which takes account of any inefficiency in the utilization of biological material due to waste or expenditure of free energy. We shall have to evaluate the growth time $t_{\text{gr}}(z) \equiv (2d \ln a/dt)^{-1}$ for organisms with $a \approx \bar{a}(z)$ at level z . The function $\bar{a}(z)$ is then given in terms of t_{gr} by

$$d \ln \bar{a}/dz = [2t_{\text{gr}}w_d(z)]^{-1}. \quad (36)$$

For the integrated column density $N(a) \equiv \int dz n(a, z)$ we also find $N(a) \approx 2t_{\text{gr}}w_d n(\bar{z})$, where \bar{z} is such that $\bar{a}(\bar{z}) = a$. The total mass contained in organisms in different size ranges is then given by

$$(4\pi a^2 d)N(a) \approx 2t_{\text{gr}}(a)\epsilon(z)R. \quad (37)$$

Assume that an organism, while drifting downward with speed w_d , can expend enough mechanical energy to acquire a horizontal velocity component of up to θw_d , where θ is some angle less than 1 radian. Its vertical speed relative to other similar organisms is about $0.5w_d$ and in time t a volume $(\theta^2/6)(w_d t)^3$ is accessible to a searching organism. When $n(z)$ times this volume is unity, the organism has a good probability of coalescing with a mate and doubling in mass. With $n(z)$ given by equation (35), the growth time is then

$$t_{\text{gr}} \approx \frac{4}{\ln 2} \left(\frac{3\pi \bar{a}^2 d}{\epsilon R \theta^2 w_d^2} \right)^{1/3}. \quad (38)$$

If $\bar{a} > a_{\text{Re}}$, we have, independent of d both for the troposphere and the mesosphere,

$$t_{\text{gr}} \approx \left[\frac{1}{\theta^2} \left(\frac{a}{1 \text{ cm}} \right)^2 \frac{175 \text{ K}}{T} \frac{P}{1 \text{ bar}} \frac{3 \times 10^{-9} \text{ 0.3}}{R} \frac{1}{\epsilon} \right]^{1/3} 20 \text{ s}. \quad (39)$$

For such organisms the troposphere is quite favorable even in the absence of photoautotrophs as prey ($R \sim 5 \times 10^{-14} \text{ g cm}^{-2} \text{ s}^{-1}$); for instance, with $T \approx 300 \text{ K}$ and $d \sim 10^{-4} \text{ cm}$, we have $a_{\text{fl}} \sim 6 \text{ cm}$ and

TABLE 2
MAXIMUM HUNTER SIZES

θ	SOURCE OF METABOLITES	
	Abiological Organic Matter	Photoautotrophs
2×10^{-3} radians.....	6 cm	40 m
10^{-1}	3 m	2 km
1.....	30 m	20 km

$a_{\text{max}} \sim (\theta/0.002)6 \text{ cm}$, so that buoyancy can be achieved with quite small values of θ . For $R \sim 3 \times 10^{-9} \text{ g cm}^{-2} \text{ s}^{-1}$, $a_{\text{fl}} \sim 6 \text{ cm}$ requires only $a_{\text{max}} \sim (\theta/3 \times 10^{-6})6 \text{ cm}$; microradian maneuverability suffices. The maximum sizes of organisms embracing the hunter doctrine as a function of the maneuverability, θ , and the source of food are given in Table 2. We see that very large hunters are permitted, within the resolution limits of the *Mariner Jupiter/Saturn* imaging system.

To derive an explicit relation between typical radius a and vertical level $\bar{z}(a)$, we must integrate equation (36) with t_{gr} given by equation (39). The result depends on whether θ is constant or a function of a . Neglecting the variations of θ , w_d , and ϵ gives (for a much larger than the original size a_1 at level Z_1)

$$Z_1 - \bar{z}(a) = 3w_d(\bar{z})t_{\text{gr}}(a). \quad (40)$$

We still have to calculate the mechanical energy expended by an organism in maintaining its horizontal hunting speed θw_d . In pure downward drift the rate of energy dissipation equals the rate of gravitational energy release mgw_d . The equivalent rate for maintaining the horizontal speed (with $\theta < 1$) is at most θmgw_d . (With judicious sailing and soaring it could be appreciably less.) The relevant quality factor is the ratio $\Delta E/\Delta m$ of mechanical energy expended in finding a partner to the increase in mass of biological material. (Biochemical energy storage is of order $10^{11} \text{ ergs g}^{-1}$ and a mechanical quality factor $\sim 10^9 \text{ ergs g}^{-1}$ is a very modest assumption.) The heat of combustion (full oxidation) of molecular hydrogen is about 10 times that of glucose and more than 3 times that of such fats as stearic acid. It is not the unavailability of reduced compounds but rather the unavailability of oxidized compounds on Jupiter which probably sets limits on the efficiency of internal metabolism of hypothetical Jovian organisms. We have

$$\frac{\Delta E}{\Delta m} \lesssim \theta g w_d t_{\text{gr}}, \quad (41)$$

which depends quite weakly on temperature and pressure. For the upper troposphere

$$\frac{\Delta E}{\Delta m} \lesssim \left(\frac{a}{1 \text{ cm}} \right)^{2/3} \left(\frac{d}{10^{-4} \text{ cm}} \right)^{1/2} \times \left(\theta \frac{3 \times 10^{-9} \text{ 0.3}}{R} \frac{1}{\epsilon} \right)^{1/3} 5 \times 10^6 \frac{\text{erg}}{\text{g}} \quad (42)$$

represents quite a modest power expenditure, except for the largest organisms. A 100 m radius hunter of photoautotrophs with $\theta = 0.01$ radian excursion capability and a 1 cm skin thickness requires a quality factor of 10^{11} ergs g^{-1} . The same quality factor is required by a 1 m radius hunter of abiological organic matter with $\theta = 0.03$ radians and $d = 1$ cm.

Even smaller power expenditures will be required if, as would be likely, evolution selects organisms with sensory systems which increase the efficiency of hunting food—such as, e.g., optical sensors for detecting chromophores. Likewise, acceleration sensors capable of detecting convective “thermals” would ease the restrictions on floater sizes and energy expenditures; and habitats near the boundaries between upward and downward convective regimes would improve the cost of Jovian biology.

The path from sinkers to hunters to floaters is an evolutionary path. It provides a possible sequence for the evolution of floaters which, as we have seen, would be difficult to understand directly from sinkers. Once floaters are established, they may be able to replicate without passing through the sinker stage at any point in their life cycles. For this to occur, of course, the minimum radius of their dispersules must be larger than a_1 .

While we have distinguished passive sinkers, hunters, and floaters in this discussion, it is clear that a single highly evolved Jovian organism might partake of qualities of all of these life styles—for example, at different stages in the life cycle. Indeed, it may be that only after the hunting doctrine is adopted by sinkers can growth to sizes large enough for the evolution of floaters become possible. We have in this discussion made no distinction among various locales on Jupiter; but it is clear that some locales—the Great Red Spot, for example—may be more favored than others because of higher abundances of organic molecules, prevailing updrafts, or other reasons.

Among other objects in the outer solar system which possess atmospheres, only Titan and Saturn exhibit colorations similar to those on Jupiter. Because of the absence of convective pyrolysis on Titan, the chromophores there can quite readily be ultraviolet photo-produced organic molecules (Sagan 1973). However, the physical environment of Saturn is very similar to that of Jupiter in the respects relevant to the arguments of this paper, and we therefore tentatively consider an airborne biota on Saturn as well.

The test of these ideas is, of course, observational. Flyby, orbital, and entry probe spacecraft each can perform significant tests of these ideas. For example, entry gas chromatograph/mass spectrometers for the near future are anticipated to have detectivities of organic matter as good as about 10^{-10} g cm^{-3} . The predicted steady-state density of complex organic

TABLE 3

STEADY-STATE DENSITY OF ORGANIC MOLECULES (g cm^{-3})

	Abiological	Biological
Lower Mesosphere.....	2×10^{-11}	9×10^{-6}
Upper Troposphere.....	2×10^{-15}	9×10^{-10}

molecules on Jupiter is RH/K_c and is roughly estimated, using the numerical values of this paper, both for the lower mesosphere and upper troposphere and for abiological and biological sources of organic matter, in Table 3. While most biological organic matter will be in organisms and not in free molecules, the densities predicted in Table 3 are sufficiently large that a high-sensitivity entry gas chromatograph may be a significant test of the biological hypotheses of the present paper. Because of the slow convective velocities of the mesosphere, such instruments should be capable of working at such pressure levels. For comparison, the density of dissolved organic matter at 2000 m depth in the north-central Pacific is equal to 5×10^{-7} g cm^{-3} , and of particulate organic matter, 3×10^{-9} g cm^{-3} (Williams and Carlucci 1976).

VIII. FINAL REMARKS

The possible existence of indigenous Jovian organisms is also relevant to the question of sterilization of spacecraft intended for entry into the atmosphere of Jupiter. Even if the ambient environment is inconsistent with the growth of microbial contaminants from Earth, the internal environment of Jovian organisms may be much more hospitable. The replication of terrestrial contaminants in the Jovian clouds also depends on the availability of trace elements. We have seen (§ III) that indigenous Na is probably missing from the upper troposphere, and that indigenous Mg must certainly be missing. Magnesium ions are essential for nucleic acid replication and a wide range of other biological functions; if Mg is missing from the clouds, the likelihood of terrestrial biological contamination of Jupiter becomes nil. However, exogenous sources of sodium, magnesium, and other trace elements, particularly from micrometeorites, while small, cannot be neglected (§ III). Consequently, it seems judicious not to exclude prematurely the possibility of biological contamination of Jupiter by terrestrial microorganisms.

This research was supported by NASA grants NGR 33-010-101 and NGR 33-010-082 and NSF grants AST 75-21153 and MPS 74-17838. We are grateful to Drs. R. Danielson, B. Draine, F. Dyson, M. Eigen, P. Gierasch, K. Hare, N. H. Horowitz, D. Hunten, A. Ingersoll, W. Irvine, J. Lederberg, J. Lewis, W. Press, R. Prinn, W. Rossow, and D. Stevenson for interesting discussions.

APPENDIX

Consider a plane-parallel slab of total optical thickness τ_0 and let $I(\tau, \mu)$ be the intensity of radiation at depth τ with μ the cosine of the angle between the propagation direction and the forward normal. Assume isotropic scattering and let ω_0 be the single-scattering albedo, which may be a function of τ . The equation of radiative

transfer (Chandrasekhar 1960; Irvine 1975) then reads

$$\mu \frac{d}{d\tau} I'(\tau, \mu) = -I'(\tau, \mu) + \bar{\omega}_0 \frac{1}{2} \int_{-1}^1 d\mu' I'(\tau, \mu') + \bar{\omega}_0 \exp(-\tau/\mu_0) \quad (\text{A1})$$

for an incident beam of unit intensity with direction cosine μ_0 , where I' is the intensity of the diffuse radiation and $\exp(-\tau/\mu_0)$ that of the attenuated incident beam. The Eddington approximation can be obtained by substituting a function of a single variable $I_+'(\tau)$ for $I'(\tau, \mu)$ when $0 < \mu < 1$ and another function $I_-'(\tau)$ when $-1 < \mu < 0$. Let

$$\kappa \equiv [3(1 - \bar{\omega}_0)]^{1/2} \quad (\text{A2})$$

and let $J'(\tau)$ be the average over all μ of $I(\tau, \mu)$. For constant κ and a semi-infinite medium ($\tau_0 \rightarrow \infty$), one finds

$$J'(\tau) = a \exp(-\kappa\tau) - b \exp(-\mu_0^{-1}\tau), \quad a = \frac{1 + (2/3)\mu_0^{-1}}{1 + (2/3)\kappa} b, \quad b = \frac{3\bar{\omega}_0}{\mu_0^{-2} - \kappa^2}. \quad (\text{A3})$$

The effective reflection coefficient $R \equiv 1 - f$, where f is the fraction of the energy flux that is absorbed, is given by

$$R = \frac{\bar{\omega}_0}{(1 + \kappa\mu_0)[1 + (2/3)\kappa]}. \quad (\text{A4})$$

Generalizations for anisotropic scattering are discussed by Chandrasekhar (1960), Prinn (1970), and Irvine (1975). For isotropic scattering Prinn used equation (A3) for normal incidence ($\mu_0 = 1$) in his numerical work. For general μ_0 but with $\kappa \ll 1$, equation (A4) reduces to

$$f(\mu_0) \equiv 1 - R(\mu_0) \approx \kappa(2/3 + \mu_0). \quad (\text{A5})$$

For many purposes one is interested only in results averaged over a whole daylight hemisphere, i.e., averaged over μ_0 from 0 to 1. Such averages are represented by the single problem we shall consider here, where the incident intensity $I_{\text{inc}}(\mu)$ equals unity for all μ between 0 and 1. In the spirit of the Eddington approximation we replace the problem by one for intensity $I(\tau, \mu)$ without explicitly isolating the attenuated incident beam: By analogy with equation (A1) we have

$$\mu \frac{d}{d\tau} I(\tau, \mu) = -I(\tau, \mu) + \bar{\omega}_0 \frac{1}{2} \int_{-1}^1 d\mu' I(\tau, \mu'), \quad (\text{A6})$$

which leads to the coupled equations

$$\frac{dF(\tau)}{d\tau} = -J(\tau)[1 - \bar{\omega}_0(\tau)], \quad \frac{dK(\tau)}{d\tau} = -F(\tau), \quad (\text{A7})$$

where

$$J(\tau) \equiv \frac{1}{2} \int_{-1}^1 d\mu I(\tau, \mu), \quad F(\tau) \equiv \int_{-1}^1 d\mu \mu I(\tau, \mu), \quad K(\tau) \equiv \frac{1}{2} \int_{-1}^1 d\mu \mu^2 I(\tau, \mu). \quad (\text{A8})$$

We again make the approximation (but here for *all* the radiation) that $I(\tau, \mu) = I_-(\tau)$ for $\mu > 0$ and $I(\tau, \mu) = I_+(\tau)$ for $\mu < 0$, so that

$$J = 3K = \frac{1}{2}(I_+ + I_-), \quad F = \frac{1}{2}(I_+ - I_-). \quad (\text{A9})$$

In this problem, any explicit consideration of the incident beam is simply replaced by the boundary condition that $I_+(\tau = 0) = 1$ and the effective reflection coefficient $R = 1 - f$ is simply given by $I_-(\tau = 0)$.

For general $\bar{\omega}_0(\tau)$ and with $\kappa(\tau)$ defined by equation (A2), the use of the Eddington approximation (A9) in equation (A7) leads to the eikonal equation

$$\left[\frac{d^2}{d\tau^2} - \kappa^2(\tau) \right] I_{\pm}(\tau) = 0 \quad (\text{A10})$$

and to the further relation

$$2\kappa^2(I_+ + I_-) = 3 \frac{d}{d\tau} (I_- - I_+). \quad (\text{A11})$$

We first solve these equations for the case of constant κ for a slab of total thickness τ_0 : We assume that the effective reflection coefficient $R_0 \equiv I_-(\tau_0)/I_+(\tau_0)$ is given as one boundary condition, the other boundary condition for the incident beam being $I_+(0) = 1$. The general solution of the coupled equations (A10) and (A11) is

$$I_{\pm}(\tau) = a\{(3 \pm 2\kappa) \exp(-\kappa\tau) - \gamma(3 \mp 2\kappa) \exp[\kappa(\tau - 2\tau_0)]\}, \quad (\text{A12})$$

with a and γ disposable constants. The requirement of $I_-/I_+ = R_0$ at the second boundary ($\tau = \tau_0$) leads to

$$\gamma = \frac{(3 - 2\kappa) - R_0(3 + 2\kappa)}{(3 - 2\kappa) - R_0(3 - 2\kappa)}, \quad (\text{A13})$$

and the condition $I_+(0) = 1$ then gives a . The final expression for the intensity J (averaged over direction cosines) is then

$$J(\tau) = \frac{3\{\exp(-\kappa\tau) - \gamma \exp[\kappa(\tau - 2\tau_0)]\}}{(3 + 2\kappa) - (3 - 2\kappa)\gamma \exp(-2\kappa\tau_0)}. \quad (\text{A14})$$

Another quantity of interest is the effective reflection coefficient R_i of the whole slab at the surface of incidence, which is $\propto I_-(0)$,

$$R_i = \frac{(3 - 2\kappa) - \gamma(3 + 2\kappa) \exp(-2\kappa\tau_0)}{(3 + 2\kappa) - \gamma(3 - 2\kappa) \exp(-2\kappa\tau_0)}. \quad (\text{A15})$$

Two limiting cases are of interest for the solutions given by equations (A12) to (A15). Consider first the case with $R_0 = 0$ in the limit of $\kappa \rightarrow 0$ with τ_0 kept finite. In this case equations (A14) and (A15) reduce to

$$f \equiv 1 - R_i = \frac{4}{3\tau_0 + 4}, \quad J(\tau) = \frac{3(\tau_0 - \tau) + 2}{3\tau_0 + 4}. \quad (\text{A16})$$

The other case is the limiting case of $\tau_0 \rightarrow \infty$ for any constant, nonzero κ . Independently of the value of R_0 , this case gives

$$f \equiv 1 - R_i = \frac{4\kappa}{3 + 2\kappa}, \quad J(\tau) = \frac{3 \exp(-\kappa\tau)}{3 + 2\kappa}. \quad (\text{A17})$$

When $\kappa \ll 1$, the value of f in equation (A17) agrees with the average over $0 < \mu_0 < 1$ of equation (A5) which is $\bar{f} = (4\kappa/3)$.

No exact solutions of the eikonal equation (A10) exist for general $\kappa(\tau)$, but if κ varies sufficiently slowly, one is tempted to use the WKB approximation. For a semi-infinite medium, only one of the two WKB solutions survives, and we have

$$J(\tau) \propto [\kappa(\tau)]^{-1/2} \exp\left[-\int_0^{\tau} d\tau' \kappa(\tau')\right]. \quad (\text{A18})$$

Note that substituting a varying $\kappa(\tau)$ into equation (A17) (or into eq. [5] of Prinn 1970, which is the equivalent of our eq. [A3] for normal incidence instead of diffuse illumination) is *not* a good approximation to equation (A18) if κ varies appreciably, even if the variation is slow. Furthermore, the requirement for the validity of the WKB approximation is that $(d\kappa/d\tau) \ll \kappa^2$, which is not satisfied by practical cases for $\kappa(\tau)$, such as the example in Figure 2. An inelegant but reliable numerical method proceeds as follows: Subdivide the total slab into a large but finite number of thin slabs (with $\Delta\tau \approx 0.3$, say) and replace $\kappa(\tau)$ for each thin slab by its average value over this slab. Start with the *last* thin slab, assume $R_0 = (3 - 2\kappa)/(3 + 2\kappa)$, and evaluate equations (A13) to (A15) with the slab thickness τ_0 replaced by $\Delta\tau$. The value for R_i obtained from equation (A15) for the last slab is then used as R_0 for the penultimate thin slab, and J and R_i are again evaluated, and so on iteratively until the *first* thin slab. The solid curve labeled J is the result of such a numerical solution for $J(\tau)$, and the effective reflection coefficient R_i for the whole medium (obtained at $\tau = 0$) is $R_i \approx 0.85$. The dashed curve is the result for $J(\tau)$ in a different problem—no absorption for $\tau < \tau_0$ and complete absorption for $\tau > \tau_0$, with $\tau_0 \approx 7.5$ (the value of τ for which $\kappa = 0.5$ in the actual problem). Equation (A16) gives the solution for $J(\tau)$ for this problem and also yields $R_i \approx 0.85$. Equation (A16) for R_i should be a fairly good solution for any $\kappa(\tau)$, with τ_0 the value where $\kappa \approx 0.5$, as long as $\tau_0 \gg 1$ and κ is small for τ appreciably less than τ_0 .

The accuracy of the numerical solution described above is limited (apart from computational errors) by errors inherent in the Eddington approximation, including the use of a constant coefficient in equation (A11). For a single slab this approximation is excellent when $\kappa \ll 1$, although other two-stream approximations are better

(Sagan and Pollack 1967; Irvine 1975) when $\tilde{\omega}_0 \ll 1$. For the problems with $\tau_0 \gg 1$, discussed here, κ is small near the incident surface and increases only slowly with τ (at first). The results for $J(\tau)$ and R_i are most sensitive to layers with moderately small τ and are insensitive to inaccuracies in the Eddington approximation at large τ .

REFERENCES

- Aitken, D. K., and Jones, B. 1972, *Nature*, **240**, 230.
 Allen, C. W. 1973, *Astrophysical Quantities* (3d ed.; London: Athlone).
 Aumann, H. H., Gillespie, C. M., and Low, F. J. 1969, *Ap. J. (Letters)*, **157**, L69.
 Axel, L. 1972, *Ap. J.*, **173**, 451.
 Batchelor, G. K. 1970, *An Introduction to Fluid Dynamics* (New York: Cambridge University Press).
 Bernal, J. D. 1967, *The Origin of Life* (London: Weidenfeld and Nicolson).
 Brown, R. 1976, *Ap. J. (Letters)*, **206**, L179.
 Carlson, R. W., and Judge, D. L. 1974, *J. Geophys. Res.*, **79**, 3623.
 Chandrasekhar, S. 1960, *Radiative Transfer* (New York: Dover).
 Elliot, J. L., Wasserman, L. H., Veverka, J., Sagan, C., and Liller, W. 1974, *Ap. J.*, **190**, 719.
 Ferris, J. P., and Chen, C. T. 1975, *Nature*, **258**, 587.
 French, R. G., and Gierasch, P. J. 1974, *J. Atm. Sci.*, **31**, 1707.
 Gierasch, P. J. 1973, *Icarus*, **19**, 482.
 ———. 1976, *Icarus*, in press.
 Gillett, F. C., Low, F. J., and Stein, W. A. 1969, *Ap. J.*, **157**, 925.
 Hogan, J. S., Rasool, S. I., and Encrenaz, P. J. 1969, *J. Atm. Sci.*, **26**, 898.
 Houck, J. R., Pollack, J. B., Schaak, D., Reed, R. A., and Summers, A. 1975, *Science*, **189**, 720.
 Hunten, D. M. 1975, in *Atmospheres of Earth and the Planets*, ed. B. McCormick (Dordrecht: Reidel).
 Ingersoll, A. P., Munch, G., Neugebauer, G., and Orton, G. S. 1976, in *Jupiter, the Giant Planet*, ed. T. Gehrels (Tucson: University of Arizona Press).
 Irvine, W. M. 1975, *Icarus*, **25**, 175.
 JANAF. 1971, *Thermochemical Tables*, 2d ed. (NSRDS-NGS37).
 Keay, C. S., Low, F. J., Rieke, G. H., and Minton, R. B. 1973, *Ap. J.*, **183**, 1063.
 Khare, B. N., and Sagan, C. 1973, *Icarus*, **20**, 311.
 ———. 1975, *Science*, **189**, 722.
 Kliore, A. J., and Woiceshyn, P. M. 1976, in *Jupiter, the Giant Planet*, ed. T. Gehrels (Tucson: University of Arizona Press).
 Lacy, J. H., Larrabee, A. I., Wollman, E. R., Geballe, T. R., Townes, C. H., Bregman, J. D., and Rank, D. M. 1975, *Ap. J. (Letters)*, **198**, L145.
 Langmuir, I. 1948, *J. Meteor.*, **5**, 175.
 Lehninger, A. L. 1972, *Bioenergetics* (2d ed.; Menlo Park: Benjamin).
 Lewis, J. S. 1969a, *Icarus*, **10**, 365.
 ———. 1969b, *Icarus*, **10**, 393.
 ———. 1976, *Origins of Life*, in press.
 Lewis, J. S., and Prinn, R. G. 1970, *Science*, **169**, 472.
 Mason, B. J. 1971, *The Physics of Clouds* (Oxford: Clarendon Press).
 Miller, S. L., and Orgel, L. 1973, *The Origins of Life* (Englewood Cliffs: Prentice-Hall).
 Morowitz, H., and Sagan, C. 1967, *Nature*, **215**, 1259.
 Noyes, W. A., Jr., and Leighton, P. A. 1941, *The Photochemistry of Gases* (New York: Reinhold).
 Orton, G. S. 1975a, *Icarus*, **26**, 125.
 ———. 1975b, *Icarus*, **26**, 142.
 ———. 1975c, *Icarus*, **26**, 159.
 Peek, B. M. 1958, *The Planet Jupiter* (London: Faber & Faber).
 Pimentel, G. C., Atwood, K. C., Gaffron, H., Hartline, H. K., Jukes, T. H., Pollard, E. C., and Sagan, C. 1966, *Biology and the Exploration of Mars*, ed. C. S. Pittendrigh, W. Vishniac, and J. P. T. Pearman (NAS/NRC Publication 1296), chap. 12.
 Prinn, R. G. 1970, *Icarus*, **13**, 424.
 ———. 1973, *Science*, **182**, 1132.
 ———. 1974, *Bull. AAS*, **6**, 375.
 Prinn, R. G., and Owen, T. 1976, in *Jupiter, the Giant Planet*, ed. T. Gehrels (Tucson: University of Arizona Press).
 Rabinowitz, J., Woeller, F., Flores, J., and Krebsbach, R. 1969, *Nature*, **224**, 796.
 Ridgway, S. T. 1974, *Ap. J. (Letters)*, **187**, L41.
 Rossow, W. 1976, Ph.D. thesis, Cornell University.
 Sagan, C. 1960, *Jet Propulsion Lab. Tech. Rept.* 32-34.
 ———. 1961, *Radiation Res.*, **15**, 174.
 ———. 1968, *Science*, **159**, 448.
 ———. 1970, *Encyclopaedia Britannica*, s.v. "Life."
 ———. 1971, *Space Sci. Rev.*, **11**, 73.
 ———. 1973, *Icarus*, **18**, 649.
 ———. 1975, *Origins of Life*, **5**, 497.
 Sagan, C., Dayhoff, M. O., Lippincott, E. R., and Eck, R. 1967, *Nature*, **213**, 273.
 Sagan, C., and Khare, B. N. 1971a, *Science*, **173**, 417.
 ———. 1971b, *Ap. J.*, **168**, 563.
 Sagan, C., and Miller, S. L. 1960, *A.J.*, **65**, 499.
 Sagan, C., and Pollack, J. B. 1967, *J. Geophys. Res.*, **72**, 469.
 Sagan, C., Veverka, J., Wasserman, L., Elliott, J., and Liller, W. 1974, *Science*, **184**, 901.
 Salpeter, E. E. 1973, *Ap. J. (Letters)*, **181**, L83.
 ———. 1974, *Ap. J.*, **193**, 579.
 Savage, B. D., and Caldwell, J. J. 1974, *Ap. J.*, **187**, 197.
 Schwarzschild, M. 1958, *Structure and Evolution of the Stars*, (Princeton: Princeton University Press).
 Shklovskii, I. S., and Sagan, C. 1966, *Intelligent Life in the Universe* (San Francisco: Holden-Day).
 Smoluchowski, R. 1973, *Ap. J. (Letters)*, **185**, L95.
 Stauffer, D., and Kiang, C. S. 1974, *Icarus*, **21**, 129.
 Stevenson, D. J., and Salpeter, E. E. 1976, in *Jupiter, The Giant Planet*, ed. T. Gehrels (Tucson: University of Arizona Press).
 Strobel, D. F. 1973a, *J. Atm. Sci.*, **30**, 489.
 ———. 1973b, *J. Atm. Sci.*, **30**, 1205.
 ———. 1975, *Rev. Geophys. Space Phys.*, **13**, 372.
 Trafton, L. M., and Munch, G. 1969, *J. Atm. Sci.*, **26**, 813.
 Vallentyne, J. R. 1964, *Geoch. Cosmoch. Acta*, **28**, 157.
 Wallace, L., and Hunten, D. M. 1973, *Ap. J.*, **182**, 1013.
 Wallace, L., Prather, M., and Belton, M. J. 1974, *Ap. J.*, **193**, 481.
 Weidenschilling, S. J., and Lewis, J. S. 1973, *Icarus*, **20**, 465.
 Westphal, J. A., Matthews, K., and Terrile, R. J. 1974, *Ap. J. (Letters)*, **188**, L111.
 Williams, P. M., and Carlucci, A. F. 1976, *Nature*, **262**, 810.
 Woeller, F., and Ponnampuruma, C. 1969, *Icarus*, **10**, 386.

CARL SAGAN: Laboratory for Planetary Studies, Cornell University, Ithaca, NY 14853

E. E. SALPETER: Newman Laboratory for Nuclear Studies, Cornell University, Ithaca, NY 14853